Czech Technical University in Prague
Faculty of Biomedical Engineering
Department of Biomedical Technology

Master's Thesis

System for dynamic cultivation of planar recellularized pericardium structures with controlled mechanical load

Rasim Muftiev

Supervisor: Ing. Roman Matějka

Study Programme: Biomedical and Clinical Technology

Field of Study: Biomedical Engineering

Declaration

I hereby declare that I have completed this thesis independently and that I have listed all the literature and publications used.
I have no objection to usage of this work in compliance with the act §60 Zákon č. 121/2000Sb. (copyright law), and with the rights connected with the copyright act including the changes in the act.

In Kladno on May 20, 2016 .....

Aknowledgements

I would like to thank my supervisor Ing. Roman Matejka for his support and advices Special throughout completion of this master's thesis. Special thanks for the consultants: Ing. Jana Zárubová, Mgr. Elena Filová, Ph.D. (IoP Acad. Sci. Czech Republic) and the material support by grant of Ministry of Health of the Czech Republic, nr. 15-29153A - Development of an aortic heart valve based on pericardium using primary and stem cells and mechanical loading in a bioreactor.

Abstract

System for dynamic cultivation of planar recellularized pericardium structures with controlled mechanical load

Decellularized pericardium seeded with adipose tissue-derived stem cells (ASCs) and human endothelial cells (HUVEC or HSVEC) is considered to be a suitable biomaterial to cultivate a living aortic valve prosthesis and improve aortic valve diseases treatment. The method includes defined values of the mechanical load on pericardium sample, which are necessary for the cell stimulation to remodel the aortic valve structure (by synthetizing collagen and other extracellular matrix components). This master thesis describes an improved cultivation system, which enables sensing the pressure values up to 300 mmHg inside the cultivation chamber as well as recellularized pericardium diaphragm's extension values in range up to 2,64% of prolongation. The hardware and software design, sensor calibration tests and tests of the system on real pericardium samples are provided. Verification of the cultivation results in the designed system have shown a significant increase of production of Collagen Type IV in the dynamic cultivated versus the static cultivated decellularized pericardium.

Keywords

Cultivation chamber, bioreactor, perfusion chamber, mechanical load, pressure transducer, tissue extension sensor, recellularized pericardium, aortic valve prosthesis, adipose derived stem cells.

Contents

List of Symbols and Abbreviations

ADC	analog-to-digital convertor
ASC	adipose derived stem cells
EGF	epidermal growth factor
ETX	binary synchronous communication's character "end of text"
FGF-1	fibroblast growth factor-1
HUVEC	human umbilical vein endothelial cells
HSVEC	human saphenous vein endothelial cells
I2C	serial inter-integrated circuit electronic bus
LRC	longitudinal redundancy check
LSB	less significant bit
MCU	microcontroller unit
mmHg	millimeters of mercury, units of pressure measurement
MSB	most significant bit
N-MOSFET	n-channel metal-oxide-semiconductor field-effect transistor
PCB	printed circuit board
PGA	programmable-gain amplifier
PVE	prosthetic valve endocarditis
PSU	power supply unit
RLC	simple electrical circuit elements: resistor (R), inductor (L), capacitor (C)
SCL	serial clock line of the I2C electronic bus
SDA	serial data line of the I2C electronic bus
SPS	samples per second
STX	binary synchronous communication's character "start of text"
SVD	structural valve deterioration
VDD	positive supply voltage

Chapter 1

Introduction

The heart is one of the most important vital organs in the human body, pumping blood throughout the whole organism. Each part of it, the aortic valve particularly, plays essential role in the normal functioning of the human heart. Aortic failure can lead to fatal consequences; hence, its timely treatment is extremely important in medical practice.

There are two types of aortic heart valve diseases – aortic stenosis and aortic regurgitation. In both cases, surgical valve replacement is the main option. In order to conduct a valve replacement operation, either mechanical valve prosthesis or bioprosthesis are used. However, both of these prosthesis have a number of limitations and possess risks for patients. Among these risks, there are valve thrombosis or systemic embolism (Cohn L.H., 2011), structural valve deterioration (SVD), or prosthetic valve endocarditis (PVE)(Cohn L.H., 2011). Moreover, the existing mechanical or bioprosthesis are not living ones and hence are not capable of self-renewal or regeneration.

Currently, there is a lack of "optimal tailor-made body's own valve prosthesis" (Filova E.,2014). According to modern scientific representations, an ideal valve prosthesis would have an endothelial surface, no early structural deterioration, longer functionality. It would also grow with the patient, would have no immune response and be naturally antithrombotic with no anticoagulation treatment thereafter (Filova E.,2014).

Scientists conclude that the type of optimal bioprosthesis can be prepared by "seeding autologous decellularized pericardium in vitro with suitable autologous cells before implantation." Decellularized human pericardium consists maily of collagen fibers; therefore, it is recognized as a promising option in growing the living bioprosthesis (Filova E.,2014). Several

types of stem cells are able to respond to the mechanical loading and synthesize collagen on decellularized pericardium. Furthermore, ASCs show a promising prospective for further differentiation into smooth muscle cells.

The main idea of this thesis is to develop a method for growing a biological aortic heart valve prostheses in artificial conditions. The pericardium prosthesis will be based on human and porcine decelluralized pericardium seeded with human ASCs and covered with human endothelial cells (Havlikova J. et al. 2014; Filova E et al. 2006). In order to grow the aortic valve prosthesis, a specially designed cultivation chamber should be modified, where necessary pressure, flow, and tissue extension conditions for the ASCs differentiation into the heart smooth muscle cell will be provided and monitored. The main property – the mechanical load in the cultivation chamber, – is expected to stimulate cells to proliferate and remodel the aortic valve construct by synthetizing collagen and other extracellular matrix components (Filova E et al. 2014).

The cultivation chamber itself has to be created and 3D-modelled in the CAD systems for further construction from biocompatible materials. It should meet the requirements of the reasonable dimensions, optimal design, non-toxicity and maximal functionality. For mechanical load control, a special controlling and tuning system should be designed. For controlling the mechanical load, the piezo-resistive pressure sensor is supposed to be used. For monitoring the stretch and extension rate of the tissue under investigation, the optical sensing element appears to be the best suitable solution. The both signals - the pressure level as well as the extension rate, - should be filtered and processed in designed hardware and developed software, consequently. Successful embodiment of the given idea has to lead to cultivation of an optimal aortic valve tissue from ASCs.

Chapter 2

Literature review

2.1 Heart valve diseases

The heart is a vitally essential human organ, standing for the whole blood circulation in the human body. Its diseases often lead to fatal consequences; hence, the proper heart disease treatment is extremely important in medical practice.

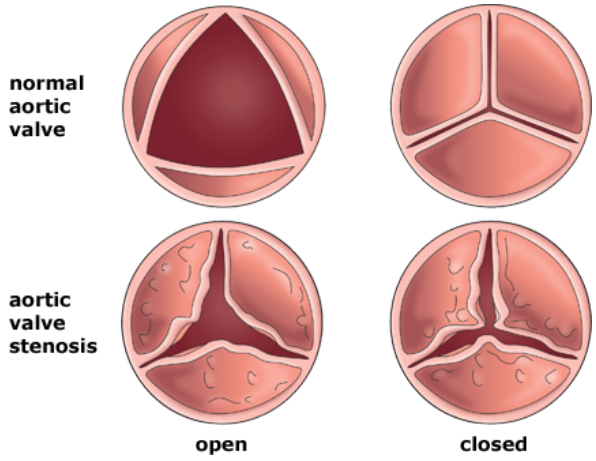

Figure 2.1: Normal aortic valve versus aortic valve stenosis.

There are many different types of heart diseases including dysfunction of the heart's blood flow and its vessels (coronary artery disease, acute myocardial infarction), heart rhythm disorders (atrial fibrillation), heart muscle disease (cardiomyopathy), heart valve diseases (valve stenosis, valve insufficiency, dysplasia), heart infections (pericarditis, pericardial effusion),

and others. This thesis is specially aimed towards heart valve diseases, mainly on the most common left heart valve diseases - aortic valve stenosis and aortic insufficiency (regurgitation).

Basically, aortic valves are a part of tightly packed connective tissue structure of the heart (Alberts et al., 2008), which is also known as the cardiac skeleton. The aortic valve lies between the left ventricle of the heart and the aorta and normally has three cusps of leaflets 2.1. The valve is responsible for the one-directional blood flow in the heart and embodies the "open-closed" mechanics due to the different blood pressure on either side of the valve.

Aortic valve diseases can be either acquired during the life of the patient or congenital (inborn). Commonly, both of the main valve diseases, aortic stenosis and aortic regurgitation, co-exist in one patient. Aortic stenosis is one of the most common and most serious valve disease problems, affecting approximately 2% of people over the age of 65, 3% of people over age 75, and 4% percent of people over age 85 (Brown J. et al, 2009). By aortic stenosis, the aortic heart valve fails to open fully, preventing the normal blood flow into the aorta from the heart. The main cause and risk of aortic stenosis development is usually calcification of the aortic valve based on the age of the patient.

Aortic regurgitation (also known as valve insufficiency or "leaky valve") is related to the inability of the aortic valve to completely close, causing the leakage of the blood back into the heart and blood contraflow. Common causes of aortic regurgitation include vasodilation of the aorta, previous rheumatic fever, infection, i.e. infective endocarditis (Brown J. et al, 2009).

Medical treatment of the aortic valve diseases can entirely be based on medications. For the severe aortic valve disease, the medical treatment involves surgical intervention including valve repair or replacement. The surgical operation leads to utilization of an aortic valve prosthesis.

Heart valve repair is technically more difficult; therefore, it is performed less often than the heart valve replacement. Heart valve replacement, especially aortic valve replacement, is an open-heart surgical procedure where the failing aortic heart valve is replaced by an artificial one.

2.2 Heart valve prosthesis

Aortic heart valve diseases are associated with high mortality rates – up to 80% at the early stages of PVE (Cohn L.H., 2011). In most cases, the only chance to treat the disease is the surgical operation, which will replace the defective aortic valve and maintain the overall functionality of the treated heart.

Recently, implantation of prosthetic cardiac valves has become increasingly common. The quality and diversity of the cardiac valve prosthesis are also growing. There are two types of valve prosthesis, particularly prosthetic aortic valves – mechanical prosthesis and bioprosthesis. Many of them possess properties that are similar to those of native valves. However, the both types of prosthesis have a number of drawbacks.

Figure 2.2: Types of mechanical aortic valve prosthesis.

Mechanical prosthesis are quite common in valve replacement surgery and they have been improving for quite a long time in medical practice (Fig. 2.2). They can actually serve up to 20 or more years in a patient's heart (Brown J. et al, 2009). Despite its functional reliability, the mechanical aortic valve prosthesis possess a number of risks and limitation for patients. Those limitations mainly refer to a valve thrombosis or systemic embolism; and therefore, a constant anticoagulation treatment, which, in its turn, leads to a risk of bleeding events. These risks are caused by the non-living properties of the mechanical aortic prosthesis; hence, resulting in an inability to cope with the formed blood clots.

Bioprosthesis, namely xenogeneic prosthesis from bovine pericardium or porcine aortic heart valves, have some distinct advantages, as they do not usually need anticoagulation

Figure 2.3: Types of bioprosthesis.

therapy after implantation (Fig. 2.3). The xenogeneic aortic valve prosthesis can last 8-10 years after implantation (Golczyk et al, 2012). A prosthetic valve from the human heart tissue, called xenograft, can also serve as an artificial valve implant. It can last almost the same time as a porcine aortic valve; however, it is used in minor cases. Despite the above-stated advantages, the bioprosthesis possess a number of risks and limitations. The main limitation is that all bioprosthesis implemented during surgery are not living in the human body; and therefore, are not capable of self-renewal and regeneration (Filova E., 2014).

Furthermore, both types of aortic valve prosthesis are associated with the risk of SVD and PVE appearance. The term SVD refers to the dysfunction or deterioration of the operated valve. SVD includes inner changes in the valve structure like leaflet calcification, leaflet disruption, retraction, fractures, etc. (excluding infections and thrombosis) (Akins C.W., 1998). PVE, on the other hand, is an endovascular microbial infection, which can appear on the implanted valve prosthesis or "reconstructed native heart valve" (Piper C., 2002). SVD, as well as PVE, are connected with a necessity for reoperation and significantly raise patients' mortality rate overall (Yankah C.A. et al., 2010).

As previously mentioned, in addition to SVD and PVE risks, both artificial prosthesis expose the human body to the risk of clot formation, thrombosis, systemic embolism (for mechanical prosthesis) and inability to live and regenerate (for both types). The reoperation rate after the implantation of a bioprosthetic is around 12.1%; whereas, the same rate for mechanical aortic valves is around 6.9% (Cohn L.H., 2011). These disadvantages of existing artificial aortic valve prosthesis led the scientists to an idea of ideal aortic valve prosthesis, which will possess characteristics as close to the real aortic valve tissue as possible. The ideal prosthetic valve should have the following properties:

- minimal or absence of insufficiency (regurgitation), namely minimal backflow of the blood through the closed valve;
- non-thrombotic property, namely liberating the patient from the anticoagulation therapy;
- ability to regenerate and self-repair;
- no immune response and low PVE rates after implantation;
- proper mechanical and physical characteristics (rate of response, minimal transvalvular pressure gradient).

The recellularized pericardium, grown in the modified cultivation chamber, should also adhere to the above-stated properties.

2.3 Stem cells usage in aortic valve prosthesis

2.3.1 Current bioprosthetic's cultivation

Current bioprosthetic aortic valves are mainly produced either from animal heart valve tissue (porcine) or animal pericardium tissue (bovine). According to the medical needs, an ideal aortic valve prosthesis should eliminate immune reactions, live, grow with the patient, regenerate and self-repair. No currently existing aortic valve prosthesis is able to self-repair; although, modern stem cell technology may provide this opportunity.

Recently, scientists have started to conduct biological experiments in order to produce artificially grown aortic valves from *autologous* (derived from the same individual) stem cells of the patient. Autologous cells are seeded on a scaffold, which acts like an artificial extracellular matrix making the artificial tissue grow in the necessary 3D structure of the original tissue, namely the aortic valve in our case. An autologous decellularized pericardium can serve as a scaffold for the growth of the prosthetic aortic valve. Decellularized human pericardium is a tough double layered heart tissue, whos main function is to provide heart protection and lubrication (Alberts B. et al., 2008). It is mostly composed of collagen fiber bundles; therefore, provides a suitable natural scaffold for "seeding in vitro with suitable autologous cells before implantation" (Filova E., 2014).

If the use of human pericardium is considered for growing an artificial aortic valve tissue and, consequently, the aortic valve, it should be mentioned that the mechanical properties of the human pericardium tissue are weaker than those of the aortic heart valve (Filova E., 2014). However, valve interstitial cells (Balachandran K et al. 2006), smooth muscle cells, bone marrow-derived stem cells (Ku C.H. et al 2006) and adipose tissue-derived stem cells (Colazzo F et al. 2011) are able to respond to mechanical loading and synthetize collagen and other extracellular matrix components, which serves as a solution to the above-stated obstacle.

2.3.2 Normal aortic valve structure. Collagen and elastin

A normal aortic valve has three cusps, which provide the normal distribution of the mechanical stress to the valve ring and aorta. The cusp is less than 1 mm thin, smooth and organized from the very few number of cells. There are 4 defined tissue layers: endothelium (continuous with aortic endothelium and ventricular endocardium), fibrosa (consists of fibroblasts and collagen fibers concentrically arranged in the cusps), spongiosa (loose connective tissue at the base of the cusps resisting the compressive forces and consisting mainly of mucopolysaccharides, mesenchymal cells, and fibroblasts), and ventricularis (consisting of elastin fibres radially arranged in the cusps) (Fig. 2.4). At the base, the cusps are attached to a "dense collagenous network called annulus" (Alberts B. et al., 2008). In this concern, two basic structural proteins, namely collagen and elastin, play a significant role in aortic valve tissue and, consequently, in growing an artificial aortic valve prosthesis.

Collagen – the most spread protein in the human body forming mainly the extracellular space and different connective tissues (Alberts B. et al., 2008). Collagen Type III and Type IV is of higher interest to this research, because these types are responsible for the arteries and the basement membranes, consequently. Collagen is represented in different densities in the heart; and therefore, it is very important for the whole heart functioning. Collagenous cardiac skeleton forms four heart valve rings including the aortic valve as well. Moreover, collagen is also the best adapted scaffold to the tissue growing and ideal for the deposition of cells, such as fibroblasts, which, on its turn, provide normal growing of the tissue.

Elastin – a rubber-like elastic protein, which is found in connective tissue and responsible for the shape of the tissue, especially after contraction or stretching. Shape retention is specifically important for the arteries, blood vessels, heart muscle and its part contractions,

like aortic valves. Mainly, the lack of elastin in the aortic valve to the aortic valve stenosis. Therefore, elastin expression should also be taken into account during the growth of the artificial aortic valve prosthesis.

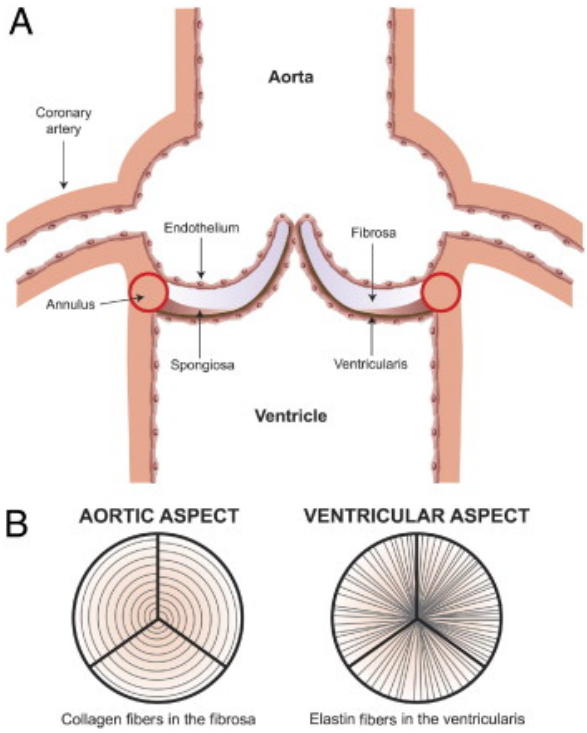

Figure 2.4: Aortic valve structure.

Furthermore, the aortic valve tissue also contains smooth muscle cells (Filova E., 2014), which should be taken into consideration during the artificial aortic valve cultivation. Additionally, endothelial tissue also covers the aortic valve. For these purpose, HUVEC or HSVEC endothelial cells should be also seeded on the pericardium scaffold.

Concluding this section, under certain conditions, adipose derived stem cells show the promising potential for the differentiation into the collagenous artificial tissue for the prosthetic aortic valve construction. The above-stated technique should allow the pericardium scaffold seeded by ASCs and HUVEC or HSVEC endothelial cells to differentiate into aortic valve tissues: collagen and elastin enriched tissues, aortic smooth muscle, and aortic endothelium.

2.4 Differentiation technique

The idea under the differentiation technique used in this research is the use of "human or porcine decellularized pericardium seeded with human ASCs and covered with human endothelial cells" (Filova E. et al., 2014). These cells can express significantly more collagen than other cell types; and moreover, ASCs show properties of better endothelialization (Policha et al., 2014). An innovative technique includes the coating of the decellularized pericardium with fibrin from both sides – inner and outer ones. Fibrin coating contains fibronectin, extracellular matrix proteins and other immobilized growth factors in it. It is used to improve the "adhesion and proliferation of ASCs" (Havlikova J. et al., 2014) and "aortic smooth muscle cells" (Filova E. et al., 2006). Another considerable factor is mechanical load. Defined values of the mechanical load aim for the cell stimulation to spread and "remodel the aortic valve structure by synthetizing collagen and other extracellular matrix components" (Filova E., et al., 2014). After the aortic valve structure is grown up, the second cultivation will be needed as long as the aortic valve structure needs the endothelial layer. Secondary fibrin coating and endothelial cell seeding embody this process (Filova E. et al., 2014).

As the result, the above-stated technique has to stimulate adipose derived stem cells to differentiate into aortic valve interstitial cells or aortic smooth muscle cells. It has to help in the endothelializition process as well. In general, the ready artificially grown up prosthetic aortic valve can be tested on a fixed stand for mechanical and biological relevance later on.

2.5 Cultivation chamber

Mechanical load is one of the mandatory prerequisites in the adipose derived stem cell differentiation into the aortic valve tissue. Mechanical load in a chamber can be produced by pressure stimulation. Hence, the cultivation chamber (bioreactor) has to possess a system for producing the pressure stimulation in a given range. In this research, the cultivation chamber is used for dynamic cultivation with mechanical load (pressure stimulation) of the flat decelluarized samples of pericardium, which will be seeded with adipose derived stem cells (ASC) and endothelial cells (HUVEC or HSVEC). Therefore, the idea behind this is to provide the planar (flat) pressure stimulation. Moreover, in order to monitor and modulate the pressure value, the controlling system for pressure stimulation of recelluarized pericardium in

chamber, including process monitoring instrumentation (flow, pressure, pulse wave), should be designed and implemented.

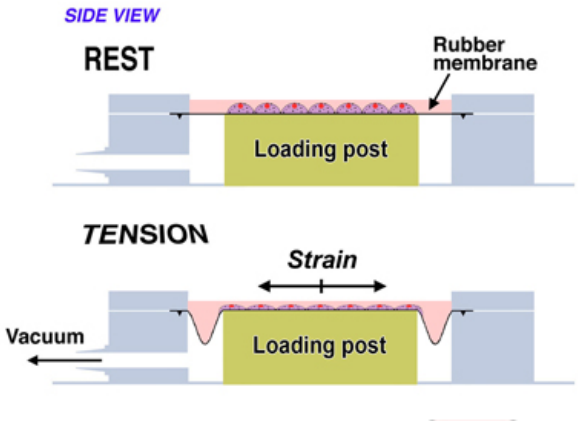

Figure 2.5: Concept of the Flexcell Tension system.

As for the existing cultivation (perfusion) chambers, bioreactors or other analogous devices, there are a few of them. Previous studies in the area of the cultivation of an artificial tissue, like aortic valve, were done on the following devices:

1. **Flexcell Tension System**. It is a computerized pressure-operated device providing defined pressure for the cells in vitro. The main part of the system is called *BioFlex culture plates 6-well culture plate*, which is used to provide the steady pressure for a monolayer culture in one or two dimensions (Fig. 2.5). It has a flexible bottom allowing the tension from the top of the plates to stimulate the pressure in the inner medium and the monolayer cultures consequently. For the complete set of the cultivation system, in addition to the *FlexCell Tension System FX4000* or *FX5000*, it is also necessary to have *BioFlex* culture plates, *Arctangle* loading stations, and *UniFlex* culture holders on top (FlexCell Inc., 2016). The properties of the *Flexcell Tension System* are represented in the Table 2.1.

2. **STREX cell strain instrument**. This device is designed to put cells under strain stress. It consists of three parts: transformer, control unit, and stretch unit. The system can set the strain value and frequency. The system also possesses the water cooling system for the stretch unit. The stretch unit itself has mechanical drive units,

Table 2.1: Flexcell system properties.

Advantages	Drawbacks
- provides defined and controlled pressure stimulation	
- well adapted to Collagen Type I and Type IV, Elastin, ProNectin and Laminin cultivation	- needs additional devices for producing the complete external pressure stimulation
- rubber membranes are optically clear for direct studying the cell with an upright microscope	- needs an additional system for tissue extension monitoring
- can be extended to up to 24 plates	- no perfusion

which produces the strain stress on the silicon chambers, where the culture under investigations is placed. The properties of the *STREX* cell strain system are represented in the Table 2.2.

3. **Existing chamber**. The existing dynamic cultivation bioreactor, designed by Ing. Roman Matejka (Matejka R et al. 2013), is already in use in the aortic valve growth experiments. The designed cultivation system is based on an field-programmable gate array's industrial controller as the main platform. The system also has online access, remote control, and a twice redundant power supply. The desired flow and mechanical parameters of the built-in perfusion system are maintained by proportionally controlled peristaltic pumps. Moreover, the perfusion system is also reinforced by a multiple-channel linear syringe pump for the complex flow and pressure pulse mode producing. The dynamic cultivation bioreactor provides a sealed enclosure for continuous sterile medium flow and usage of chemical substances within these medium, including antibiotics, growth factors, etc. For the holding of the recellularized pericardium samples inside the bioreactor, there are specially-designed silicon cultivation chambers. These chambers provide both the living conditions and the mechanical stress that is necessary for developing aortic valve tissue. All parts of the dynamic cultivation system, which are in contact with cultivation media, tissues and living cells are made from non-toxic materials, such as aluminum, silicone, santoprene, or some similar materials. All of these materials are suitable for sterilization with an autoclave or other chemical and

Table 2.2: Strex cell strain properties.

Advantages	Drawbacks
- provides pressure stimulation with defined ratio, waveform, and frequency	- non-computerized system with mechanical strain provision - has a risk of overheating inside the strain unit - cells can be investigated under a microscope only after the procedure - needs additional system for tissue extension monitoring - no perfusion

Table 2.3: Existing system properties.

Advantages	Drawbacks
- computerized system for complex data acquisition - pressure stimulation with defined ratio, waveform, and frequency - cells investigation under microscope and via Internet - perfusion maintenance and control	- needs additional system for tissue extension monitoring - needs additional system for pressure monitoring

radiation sterilization, which minimizes the risk of contamination during some long-term experiments. The main characteristics of the existing cultivation chamber are as represented in the Table 2.3.

It was already planned from the beginning, that this system would also contain several types of transducers and sensors, i.e. flow, pressure, temperature sensing, conductivity, pH, pO2 and other necessary parameters for maintaining stable living conditions in further modifications.

To combine the advantages and to reduce the number of drawbacks of the above-stated bioreactors, cultivation chambers, and plates, this master research concludes in optimizing

the perfusion chamber of Ing. Roman Matejka, which is used for flat decellularized samples of pericardium, allowing reseeding with ASCs and HUVEC or HSVEC and its further differentiation into an aortic valve prosthesis. The perfusion chamber should possess the pressure control system as well as an extension sensing system for the pericardium sample under investigation.

Chapter 3

Research gap / Main aims

The idea to grow an artificial aortic valve has captured the scientific mind. Currently, there have been successful attempts to differentiate the ASCs into the collagen and elastin enriched tissue covered by artificially grown endothelial cells. There are even a couple of designed cultivation chambers (bioreactors). This thesis focuses on improving the existing cultivation chambers for the pericardium scaffold seeded by ASCs and HUVEC or HSVEC endothelial cells, which should differentiate into aortic valve tissues.

The first aim of this thesis is to **optimize** the design of cultivation chamber (bioreactor) used for flat decellularized samples of pericardium allowing reseeding with adipose-derived stem cells (ASC) and endothelial cells (HUVEC or HSVEC).

Secondly, the aim of this thesis is to **improve** the existing differentiation method by introducing the dynamic cultivation with mechanical load (pressure stimulation) delivery and control system (flow, pressure, pulse wave).

Moreover, in order to provide a deeper understanding and analysis of the differentiation process, this thesis aims to **design** a method allowing extension sensing of recellularized pericardium diaphragm fixed in-chamber during the dynamic cultivation.

The above-stated improvements concern, technically, the cultivation chamber (or bioreactor). However, the main goal of the thesis is to **support** the improved technique of adipose derived stem cells differentiation into the into aortic valve interstitial cells and aortic smooth muscle cells and **verify** the results of cultivation in the designed system compared with static cultivated culture on decellularized pericardium.

Chapter 4

Methods

4.1 Cultivation chamber (bioreactor) description

A cultivation chamber, also known as a perfusion chamber or a bioreactor, presents the main placement, where the differentiation of ASC and endothelial HUVEC or HSVEC cells into a prosthetic aortic valve tissue is carried out. The cultivation chamber provides the sealed room for the reseeded pericardium sample stationing, filling it with a necessary medium for an adequate biochemical environment, stimulation of a sample with pressure, monitoring and investigating it with microscope, pressure sensing, tissue extension sensing, etc (Fig. 4.1). There is already an existing model of the cultivation chamber, designed by Ing. Roman Matejka (See the "*Cultivation chamber*" subchapter). The existing cultivation chamber has many advantages; however, it can be improved according to the main objectives of this thesis. The main objectives is to optimize the design of cultivation chamber used for the flat decellularized samples of pericardium with an adding controlled pressure stimulation and pressure monitoring system. The improved system of ASCs differentiation into the aortic valve interstitial cells and aortic smooth muscle cell technique should be also reinforced by an extension sensor development. The extension sensor will be used for tracking the pericardium sample extension (stretch) rate in order to investigate the most effective aortic tissue growth conditions in the cultivation chamber.

As the general structure of the cultivation chamber can be seen on the Figure 4.1, cultivation chamber consists of several essential parts. The main structural unit is a cultivation chamber (bioreactor) itself. It provides the sealed area for a pericardium sample seeded with ASC and endothelial cells. The sample is attached to the inner chamber mountings and

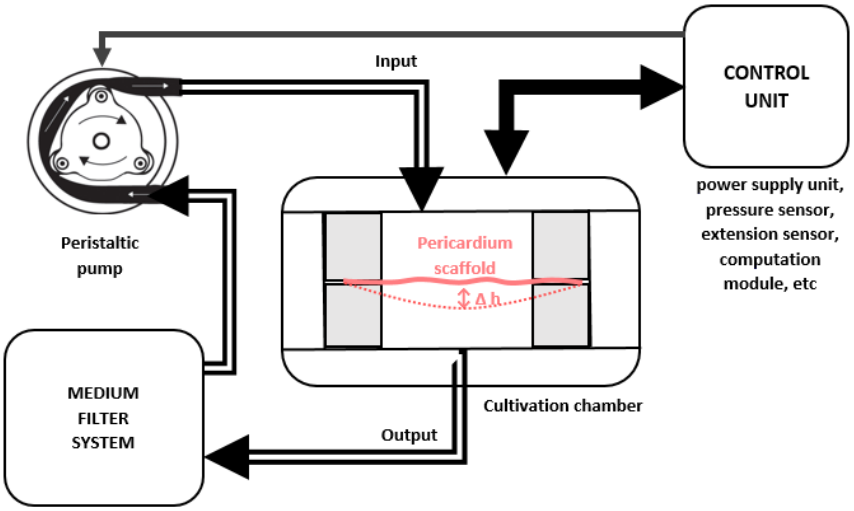

Figure 4.1: Cultivation chamber general structure.

fixed by four screws on corners, so that the wider pericardium sample area could be affected by pressure and medium stimuli. The pressure is produced by flow of an inner medium, providing a stretch tension into the tissue sample. That makes cells start actively growing a tissue with an extracellular matrix, enriched with collagen, elastin proteins, endothelial layer and other aortic valve cells.

Another essential part of the cultivation chamber is the medium system, serving for medium inner maintenance and flow under given conditions. The medium flows over a flexible rubber tube in and out of cultivation chamber. The flow is produced by an external peristaltic pump, which produces compress movements of the medium fluid by positive displacements of sprung rollers, which are affecting the inner installed flexible tube. The medium flowing from the peristaltic pump enters the cultivation chamber‘s inner room to effect the tissue sample under investigation. Further on, at the output of the cultivation chamber, there is a medium filter installed. The filter helps to provide an automatic filtration of the medium output and to substitute it by necessity. Medium substitution is made to ensure the given conditions of the medium by time and its impact on the tissue under investigation. The complete system should also assure the sealed and safe connections in the tube attachments in order to prevent leakage. All inner parts of the cultivation chamber including screws, mounting, pericardium placements, and others should be disinfected and sterilized by an autoclave in temperatures over 160°C.

Activation and work of the peristaltic pump should be manually or automatically controlled for switching on and turning off. For that purpose, there is a control unit designed. It represents an external device with the wires connected to the cultivation chamber and peristaltic pump. Moreover, the control includes the essential power supply unit (PSU), which provides the +3V3, +5V, +12V, +24V and ground voltage rails. In this thesis, the pressure stimulation and monitoring system as well as the extension sensing system will be also integrated into the control unit. The control unit includes programmed microcontrollers (MCU) to receive, compute, manipulate, and recalculate the obtained data into the user-friendly form, support further communication with computer and data transfer.

4.2 Pressure sensor hardware

4.2.1 Pressure sensor design

According to the differentiation method, used in this thesis research, mechanical load makes a significant contribution into the collagen expression of the ASC and endothelial HUVEC or HSVEC cells. A proper mechanical load application should promote the adequate and active growth of an aortic valve prosthetic tissue in the cultivation chamber. Therefore, the design of a mechanical load delivery and monitoring system becomes of higher importance. As a source of the mechanical load, normal pressure produced by flowing medium will be used. It can vary in a range from 0 mmHg to 300 mmHg. The pressure can be controlled; and it provides necessary mechanical stress to the seeded ASC and HUVEC or HSVEC on a pericardium scaffold. For the flow production, a standard peristaltic pump was used. In order to monitor and control the perfusion rate in a closed cultivation chamber and the flow pressure, consequently, an appropriate hardware design of a pressure sensor was developed. The block-scheme of the developed pressure sensor hardware can be seen on Figure 4.2.

As it was already described, the cultivation chamber (CC) is filled with an active medium (Fig. 4.2), which is pumped by a peristaltic pump and filtrated during the cultivation process in a special medium filter unit. Pressure sensor should be integrated into the medium system. In this scenario, an installed sensor can be also enveloped by medium and could deliver precise measurements. Inhomogeneity of the medium fluid, especially air bubbles, can serve as a capacitance, which badly influences on the pressure values. This all can produce inaccuracies in the performed measurements. In this case, it is essential to ensure the homogeneity of

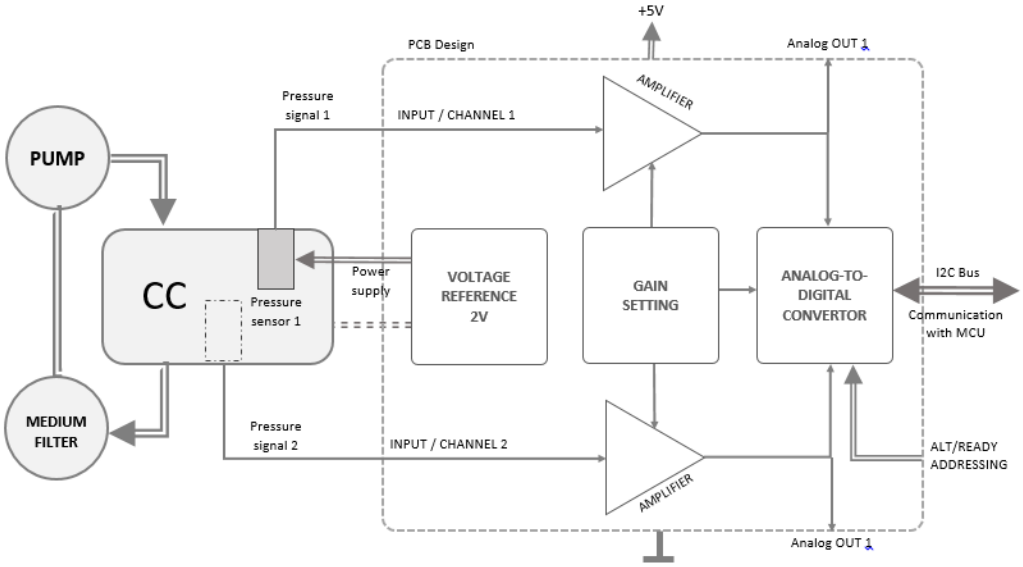

Figure 4.2: Pressure sensor structure.

the medium fluid in the system. Another solution can be an additional pressure sensor in the other part of the cultivation system or medium system. This solution could verify the equality of the pressure value in the whole medium system and ensure the reliable pressure delivery to the pericardium sample consequently. Therefore, the hardware is designed as a two-channel pressure sensing system.

The pressure sensors are usually finely tuned and precise sensing elements; and they do need a precise and stable voltage supply. Therefore, there is a +2V voltage reference block designed in the hardware. It produces the precision voltage reference serving solely for the pressure sensor's power supply. All other electronic components of the hardware are supplied from the +5V external power supply. A pressure signal from the sensor installed into the cultivation chamber enters the hardware in an analog way via a wire and should be firstly amplified so that it can be further manipulated. Two instrumental amplifiers (one amplifier on each channel) provide the necessary amplification of the analog signal. After the amplification, the signal goes to an analog-to-digital convertor (ADC), which transform the analog pressure signal into a digital one according to the preset bit rate and input voltage range, called full-scale, of an ADC. Alternatively, the analog pressure signal can be also read out in the analog way via an additional analog output of the hardware system. In the ADC, there is usually also a possibility to amplify an input signal. Although, amplification

is usually not that strong as in an electronic amplifier. The ADC amplification can be turned on and set to some value by the setting its inner registers. This can be done during a communication session with a computer, microcontroller, or other external device via I2C serial bus. The I2C is a multi-slave input-output serial computer bus, which is also present in the ADC design to provide the both-way communication and digital pressure signal transmission. Moreover, the ADC has an addressing input, ADDR, for I2C slave address selection, and an ALT/RDY output for digital comparator or signaling of the conversion readiness.

The gain (range between the input and output signals) of the amplifiers and ADC are set by corresponding methods - either by the resistor values (for amplifiers) or inner register settings (for ADC), – in order to provide a necessary output voltage range. However, the output pressure signal range is dictated by its further transmission via I2C bus to the computer and consequent calculations.

The designed hardware system has two channels. The data processing in each channel is the same. After the amplification each of two channel signals enters the ADC for further digitalization. At the ADC output, signal of each channel can be selected via I2C bus as well.

The complete pressure sensing system should also provide the safe and adequate power supply to the all system elements. For this purpose, there is +5V and build-in +2V voltage rails in the designed hardware. The electrical system should adhere to the electrical safeties regulations, paying especial attention at the in-medium-power-supply connections.

4.2.2 Pressure transducer

In a variety of electronic components and sensors, the choice of electrical elements and their interconnections should adhere to the standard electrical circuit rules and best practices of the electrical engineering. In order to provide the best available solution for signal processing, the sensing element given below was chosen.

SCW Medicath Disposable Pressure transducer is a certified disposable pressure sensor (Fig. 4.3), which main purpose is to serve for procedural blood pressure measurements in medical practice. The sensor itself represents an electrical structure with a Wheatstone bridge structure with a piezo-resistive element in it, which serves as a pressure-sensing element. It is enclosed in a plastic package, which provides a sealed space with an access via a

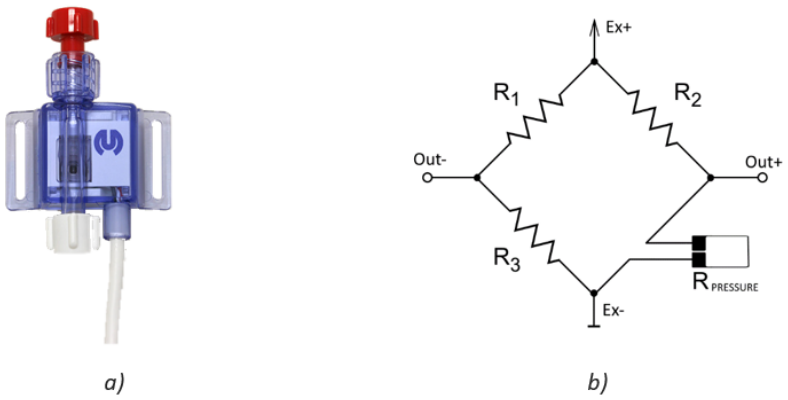

Figure 4.3: SCW Medicath pressure transducer.

tube to the medium flow (Fig. 4.3). The pressure transducer delivers precise pressure measurements and ensures the lowest possible zero drift. However, the best electrical practice declares the usage of some stabile and precise power supply of the pressure sensor on order to get the most reliable measurements.

In general, the ACCUTRANS Disposable Pressure transducer has five pins serving as follows:

- Excitation+ pin (Ex+) stands for the positive power supply of the inner electronic structure of the sensor
- Excitation- pin (Ex-) stands for the negative power supply of the inner electronic structure of the sensor, which in our case is connected to GND rail.
- Out+ pin stands for the positive signal output of the pressure sensing signal. This signal will be the pressure value, which is used and manipulated in order to obtain the final pressure value.
- Out- pin stands for the negative signal output of the pressure sensing signal. In our case, it is connected to GND rail.
- NC pin is not connected or connected to GND rail.

However, before the decision making about the SCW Medicath Disposable Pressure transducer implementation, several test with the pressure transducer were conducted (See the "*Pressure sensor's calibration test*" subchapter). The test were performed on order to prove

the linear dependency of the pressure transducer's response, its dependence from the input voltage excitation, dependence from the inner medium, as well as calibration and sensitivity of the pressure measurements. During the tests, the random two pressure transducers were selected out of several dozens. The pressure was tested within two mediums: air and liquid (water). The pressure itself was produced by the precise pressure delivery system. After all the test measurements with different voltage power supplies, the average sensitivity amounted to 0,005075±0,000036 mV/mmHg/V (millivolts per 1 mmHg of pressure per 1 Volt of power supply).

4.2.3 Other electronic components

As basics of the electrical circuit, standard RLC electronic elements, namely resistors, inductors, and capacitors of 1206 series were used. Resistors were mainly used as voltage dividers, pull-up resistors, gain setup resistors, and current limiters. Capacitors were implemented into PCB primarily in order to filtrate the power supply noises and provide better measuring results. Inductors were not necessary and therefore were not introduced in the PCB design. For external power supply and input-output signal transmission, WAGO-256 connectors and standard male pin 2.54-mm-spaced headers were used.

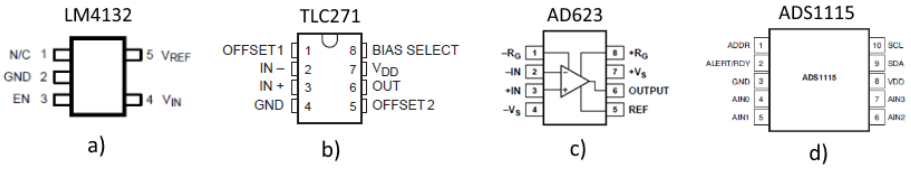

Figure 4.4: Pressure sensor's electronic components.

LM4132 voltage reference is a representative of the precision voltage references' electrical component produced by *Texas Instrumentations* (Fig. 4.4a). The reference voltage produces stabile and precise power supply of 2V. It has low temperature coefficient and low supply current – 60 μA. However, the voltage reference can produce up to 20 mA current output. These parameters are optimal for the pressure sensor's power supply and should provide the precise and stabile pressure measurements. For even better voltage reference performance and noise suppression, the input and output capacitors with values up to 10 μF are usually used.

TLC271 operational amplifier is a programmable low-power operational amplifier (Fig. 4.4b). Usually, small sensor like pressure transducer delivers output signal of a small voltage range. That leads to the fact that after the sensor measures a pressure value and process signal to the hardware, the signal should be somehow amplified in order to provide more reasonable and accurate further signal processing and decrease the rate of noise distortion. For this purpose, TLC271 amplifiers are introduced into the hardware design. The TLC271 electronics are designed for single-supply operations with a low-noise (high-bias) mode and with common-mode input voltage extending below the negative rail. The TLC271 amplifier has a high impedance input and additionally offers the bias select mode. As an operational amplifier, its gain can be set by the ratio of the resistors on its negative feedback line. However, the more exact calculations, a choice of the resistor values and the gain set, consequently, will be done only after experiments of the sensor test and output signal requirements.

AD623 instrumentation amplifier is a single supply, rail-to-rail, low cost instrumentation amplifier (Fig. 4.4c). The AD623 amplifier possess good low-noise and high DC accuracy performance characteristics. Gain of the amplifier can be set only by one external resistor and can vary from 1 up to 1000. AD623 is specifically adapted for the low power medical instrumentation usage, transducer interfaces, and low power data acquisition – the properties, which accurately suit the task of the pressure measurements in a small biological environment of the cultivation chamber.

ADS1115 analog-to digital convertor is an ultra-small, low-power, 16-Bit analog-to-digital convertor (ADC) with internal reference (Fig. 4.4d). It is specifically adapted to applications in portable instrumentation, consumer goods, temperature and other measurements. Moreover, this electronic component has been chosen due to its advantageous characteristics and suitability to the given task of the precise signal processing and digitization of pressure measurements in a cultivation chamber. In that concern, the ADS1115 has two differential or four single-ended signal inputs, wide supply range from +2V up to +5V, low current consumption (about 150 μA), programmable data rate from 8 up to 860 samples per second (SPS), internal low-drift voltage reference, and programmable comparator. Furthermore, the ADS1115 convertor possesses an internal programmable-gain amplifier (PGA). The PGA can vary from 2/3 up to 16, what gives us opportunity to process and amplify signal in the ADC decreasing the load or even a necessity in an external amplifier. Three bits in a configuration register usually set the PGA of ADS1115 convertor, which also

predefines the ADC's full scale input. The full scale input is the input signal's voltage scale, which will be converted into the digital values from 0 up to 2 bits value. In our case, the full scale of the ADS1115 will be set at the value ±2.048V. However, the input pressure signal will have to be amplified to these range by an external amplifier TLC271.

As for the output of the ADS1115, there are serial data line (SDA) and serial clock line (SCL) pinouts for an inter-integrated circuit (I2C) electronic bus connection. The I2C electronic bus is a multi-master, multi-slave serial computer bus. It uses bidirectional open drain lines allowing the master-slave communication of a microcontroller, computer, or other master device with a slave-device, which is an ADS1115 analog-to-digital convertor in our case. A master-slave communication is normally conducted via 8-bit address space; the ADS1115 is of the same kind. The master provides a clock signal on the SCL pin and data are transferred via the SDA pins. The serial lines are usually pulled up with resistors. All the basic communication configurations of the I2C interface should be initially preset. The ADS1115 can perform only as a slave device. So, the first byte sent by master should be the ADS1115 address followed by a bit, which will instruct the ADC to listen for a subsequent byte. All read and write transactions of the ADC must be initialized by a start condition (or so called acknowledge bit) and terminated by a stop condition (ADS1115 Datasheet, 2016).

The ADS1115 have four registers that are accessible via the I2C port: *Conversation*, *Config*, *Lo_thresh*, and *Hi_thresh* registers. The *Conversion* register contains the result of the last conversion in binary twos complement format. The *Config* register allows the user to change the ADC operating modes, like data rate, PGA setting, comparator mode, etc., and query the status of the devices. Two registers, *Lo_thresh* and *Hi_thresh*, set the threshold values used for the comparator function. All four registers are accessible via the Pointer register, which has to be initially set to lead to the necessary register.

There is also a ALERT/RDY pin on the ADS1115 analog-to-digital convertor. This pin is used for the internal customizable comparator, which can produce an alert signal on the ALERT/RDY pin. The build-in comparator can be used either as a traditional comparator or as a window comparator by presetting the ADC via register pointer setup. In a traditional mode, the ALERT/RDY pin is activated if conversion data exceeds the limit set in the high threshold register. In a window comparator mode, the ALERT/RDY pin is activated if conversion data exceeds the high threshold limit or falls below the low threshold limit. The high and low threshold limits are preset during an initial register pointer's setup. In this

master thesis, the comparator mode and the ALERT/RDY pin will not be used; however, it can be used in further pressure sensor usage as far as the hardware design contains the ALERT/RDY output.

The ADS1115 has also one address pin, ADDR, which sets the I2C-slave address. The pin can be connected to the ground (GND), positive power supply (VDD), SDA, or SCL, which makes the ADS1115's slave address to be selected to one of four addresses. The state of the address is sampled continuously. The ADDR pin in the experimental hardware design is connected to the GND, which sets the ADS1115 address to 7-bit form of 100 1000 binary number. However, the regular design of the pressure sensor hardware possesses special input pin for the ADDR selection, so that the ADC address could be changed in further researches or similar.

4.2.4 Initial setup of the I2C electronic bus

According to the I2C communication between MCU and ADS1115 described above, the inner register addresses and datasheets of these electronic components, for our case, it is necessary to set the ADS1115 to the continuous conversion mode firstly and then read out the conversion results. Therefore, the initial bytes sent by the MCU to the slave ADS1115 should be as following:

1. Writing to Config register.

    - the first byte set the ADS1115 address: **0100 1000** in binary form or 0x48 in hexadecimal form , where there are 7 bit of I2C address followed by a low "Read/Write" bit. In our case, the last bit is set to "Write" state.
    - The second byte switches the ADC's Pointer register to the Config register by sending **0000 0001** in binary (0x01 in hexadecimal form) byte and activates it.
    - the third byte and the forth bytes set the ADS1115 Config register parameters, which will ADS working parameters. The third byte is the most significant byte (MSB) of the Config register setup. It should be **1000 0100** in binary form or 0x84 in decimal form, because:

      - Bit 15 (operational status / single-shot conversion start): 1 - start of a single conversion;

- Bits 14:12 (input multiplexer configuration): 000 - AINP = AIN0 and AINN = AIN1 (default).

- Bits 11:9 (programmable gain amplifier configuration): 010 - full scale of ±2.048V (default).

- Bit 8 (device operating mode): 0 - continuous conversion mode.

- The third byte is the less significant byte (LSB). It should be **1000 0011** in binary form or 0x83 in decimal form, because:

- Bits 7:5 (data rate): 100 - 128 samples per second (default).

- Bit 4 (comparator mode): 0 - traditional comparator with hysteresis (default).

- Bit 3 (comparator polarity): 0 - active low (default).

- Bit 2 (latching comparator): 0 - non-latching comparator (default).

- Bit 1:0 (comparator queue and disable): 11 - disable comparator (default).

2. Setting the pointer register to conversion mode

   - The first byte is as usual the ADS1115's slave address of **0100 1000** in binary form (0x48 in hexadecimal form) followed by a low "Read/Write" bit.
   - The second byte sets the Pointer register to the Conversion register, which contains the results of last conversion, and activates it by sending the **0000 0000** in binary form (0x00 in hexadecimal form).

3. Reading out the Conversion register

   - The first byte sets the ADS1115's slave address of **0100 1000** in binary form (0x48 in hexadecimal form) followed by a high "Read/Write" bit.
   - The first incoming byte from the ADS1115's Conversion register is the most significant byte of the last conversion made.
   - The second incoming byte is the most significant byte of the last Conversion made.

These bytes have to be taken into consideration while initializing the microcontroller-ADC communication and obtain the data from the pressure transducer. The received data is than processed either in the MCU or computer.

4.2.5 Power supply unit

The already existing cultivation chamber has a ±24V power supply and consequent voltage rail. As it was stated in the "Pressure sensor design" subchapter, the designed hardware for the tissue extension's sensing requires +5V or +3V3 power supply. Therefore, the special 24V-to-5V transformer was designed and added to the designed hardware for the +5V voltage power supply (See the Appendix D for the electrical circuit diagram). The input of the transformer is attached to the +24V rail of the existing cultivation chamber via the 25 pin connector. The power supply's On/Off modes are controlled with a standard switch button on the designed enclosure box.

4.2.6 Common-mode voltage

During preliminary tests of the pressure sensor on a breadboard, the problem of common-mode voltage on the input of the AD623 instrumentation amplifier was established. Pressure transducer's Out+ output was connected to a AD623's positive input and pressure transducer's Out- output to a AD623's negative input. Whereupon, the output of the instrumentation amplifier was connected to two input channels of the ADS1115. However, according to the test measuring, there was only 7 mV in both instrumentation amplifier's outputs with no or almost no change in sensing voltage by changing the pressure value in the system. That happened due to the common-mode voltage issue.

Common-mode voltage is a voltage offset, which is present in both the inverting ("+") and non-inverting ("-") inputs of the instrumentation amplifier (John G. et al., 1999). Although the AD623 is an instrumentation amplifier, which amplifiers the difference of the input voltages, the common-mode voltage of its output with 7 mV value was due to a negative low rail. Amplifier's output could be approximately +10 mV above the low rail, which means +10 mV by GND (0 V) – pressure transducer's negative output. In that case, the AD623's output after an amplification of 300 mmHg pressure signal could be only 3 mV.

In order to eliminate the problem of the common-mode voltage on the AD623's inputs, a virtual ground was created in the hardware design. The virtual ground with value of 107,6 mV is produced by a voltage dividing *R2* (1 kΩ) and *R3* (22 Ω) resistors on +5V power supply and TLC271 operational amplifier (Gain = 1) in the pressure sensor hardware design. The virtual ground was connected to the reference input, REF, of the AD623 amplifier. The REF input defines the zero output voltage and is especially useful, when bipolar signals are

being amplified and the "load does not share a precise ground with the rest of the system. It provides a direct means of injecting a precise offset to the output" (AD623 Datasheet, 2016). Consequently, after the amplification with virtual ground connection, there will be an amplified output between Out and Ref and between Out and GND; whereupon, this value will be raised by 107,6 mV above.

The virtual ground value was also taken into consideration into the software calculations of the pressure value, namely the pressure value is corrected by the voltage offset value of 107,6 mV during the calculations.

4.2.7 Nominals of pressure sensor's electronics

According to the electronic component's choice and power supply for the pressure sensor's hardware design, there are several electronic components, mainly the RLC electronic elements, which nominals should be calculated and adjusted to provide the adequate hardware functioning. Therefore, according to the set ADC full-scale range of ±2,048V and the single +5V supply operations in the designed hardware, the sensor output after the acquisition and amplification should not exceed the range from 0 to ±2,048V on the input of the ADC. With respect to this fact, there are several resistors' and capacitors' nominals, which are setting the amplification gain and the voltages, described below. According to the conducted initial calibration test of the pressure transducer (See the "Pressure sensor testing" subchapter), the sensed pressure value by +2V power supply from the LM4132 voltage reference and maximum 300-mmHg pressure value is about 3 mV (See Table 5.2). However, after the signal from the pressure transducer enters the AD623 instrumentation amplifier, it is being altered by the solution against the common-mode voltage, namely, it is raised by value of 107,6 mV of the virtual ground taken from the REF pin of the AD623. Thereafter, the AD623 also serves as the differentiation amplifier, which gain is set by the nominal of the *R1* resistor. The system should provide the gain (G) according to the following formula:

$$G \leq \frac{V_in}{V_out} = \frac{2,048V}{3mV} = 682 \tag{4.1}$$

$$R_1 \leq R_G = \frac{100k}{G-1} = 146\ \Omega \tag{4.2}$$

According to the AD623's datasheet, its gain is calculated as in the formula (4.1). Therefore, a resistor with a nominal of the *R1* = 150 Ω from the E12 resistor's series was selected for the gain setting. The AD623's gain amounted to 667.

As it was described above, the virtual ground with value of 107,6 mV is produced by a voltage dividing *R2* and *R3* resistors with nominals 1 kΩ and 22 Ω respectively for +5V power supply. The gain of the TLC271 operational amplifier is set at the value of 1 by excluding resistors on its negative feedback line.

Moreover, according to the datasheets, the nominals of the *C1* and *C2* capacitors are chosen with values 10 μF and 1 μF respectively for the better power supply's noise suppression (LM4132 Datasheet, 2016). Similarly, the *C3* and *C4* capacitors have nominals of 100 nF for more stable power supply of the instrumentation and operational amplifiers.

4.3 Extension sensor hardware

During the differentiation technique of a pericardium sample, the growing tissue will be affected by pressure, which should stimulate the cells to increase the production of collagen and elastin proteins, as well as other aortic valve molecules. However, in order to investigate the reaction of the sample to the delivered pressure and effectiveness of the applied differentiation techniques , it is vitally necessary to monitor the deformation of the growing tissue during pressure stimulation in the cultivation chamber. However, the pericardium sample, growing collagenous structure can possess different stiffness properties, which affect the stretch rate. These facts lead to the necessity of a tissue or sample extension sensor, which will be able to deliver precise information and calculate the tissue extension value under a given pressure in the cultivation chamber.

4.3.1 Extension sensing method

There are different possibilities how to sense the extension of a tissue. However, for extension sensing method in our case, there were strict requirements of not disturbing the **sealed and sterile** inner environment of the cultivation chamber.

In that concern, the best sensing possibility is related to optical methods, namely optical sensor usage. In this master thesis, the method of a light reflection was used. For better light reflection, there is a source of light, which is represented by a light-emitting diode (LED) in

our construction. The light from the LED is emitted towards the tissue under investigation. Part of the light is dissipated, some part of it is refracted and transmitted, and some is reflected from the medium-tissue boundary back. The latter is sensed by an optical sensor, which produces an analog electrical signal according the reflected light absorption. The intensity of the reflected light is also dependent on the distance between the diaphragm, where the pericardium sample is installed, and the base line of a sensor. Consequently, the tissue extension can be recalculated as "reflected light ratio ⇒ distance to the baseline ⇒ tissue extension". However, empirical tests should be done in order to find the dependence and calibrate the informational signal versus recalculated values of the tissue extension.

Moreover, both the LED and the optical sensor should be built-in into the cultivation chamber as close to the tissue under investigation as necessary. Therefore, some construction changes were also introduced into the cultivation chamber design.

4.3.2 Extension sensor design

As it can be seen from the extension sensor's block-scheme on the Figure 4.5, there is a designed cultivation chamber (CC) with a medium flowing inside of it. The more detailed description of the cultivation chamber is given in the "*Pressure sensor design*" subchapter.

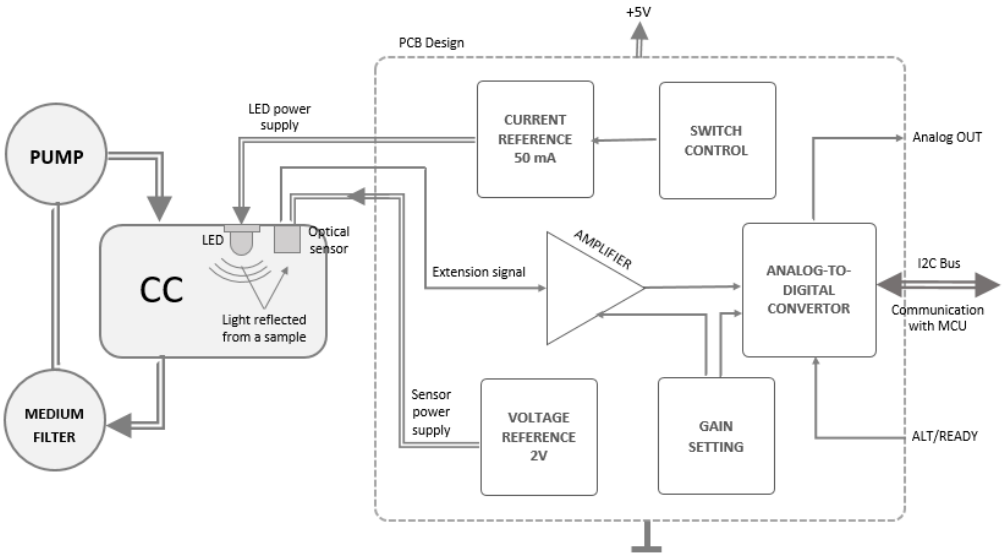

Figure 4.5: Extension sensor's structure.

The plugged into the cultivation chamber extension sensor will be connected to the hardware, specially designed for the extension sensor power supply and signal processing. In the hardware, a current reference and a switch block represent the power supply unit. The current reference produces the stable current limited to the 50 mA, the standard maximum of the implemented LED, and ensures the stabilized and steady light emitted by LED.

However, the sensing part is an accurate device, which also requires the stabile power supply in order to obtain precise and stabilized extension informational signal. For this purpose, there is a voltage reference block. It provides stabile and precise +2V power supply in order to ensure the steady and stabilized work of the optical sensor.

As an analog informational signal from the sensor enters the hardware via wires, it should be amplified. An amplified signal can be easier processed and undergoes less noise distortion. Especially for this purpose, there is an operational amplifier designed in the extension sensor hardware, which should provide signal amplification in up to 1000 range.

Further on, the amplified analog signal proceeds into the analog-to-digital convertor (ADC). ADC transforms the analog informational signal into a digital one according to the preset bit rate and input voltage range of an ADC (so called full scale). Alternatively, the designed hardware system provides a possibility to read out the analog amplified signal in the analog way via an additional analog output of the hardware system. Usually, inner ADC electrical design allows amplifying an input signal as well. However, the inner gain range of the ADC is usually much smaller than the gain range of an external operational amplifier. Anyway, the informational signal amplification during its processing in the operational amplifier and the ADC should be calculated and set by a special gain-setting block.

For the further signal proceeding and data transmission, ADC has an I2C serial computer bus. These pins work as a multi-slave input-output to provide the both-way communication between the ADC and computer or an external microcontroller. Moreover, the hardware possesses an ALERT/RDY pin for the ADC input. This pin is used for the internal customizable comparator, which can produce an alert signal on these pin.

The whole hardware could be supplied by +5V or +3V3 and GND power supply. Additionally, there is a build-in +2V rails, which is supplied by +5V. Overall, the designed hardware should provide stabile and precise informational signal of the light reflected from the sample tissue under investigation. From this informational signal, it should be possible

to recalculate the tissue extension value. The results of this assumption will be provided in the *Results* chapter.

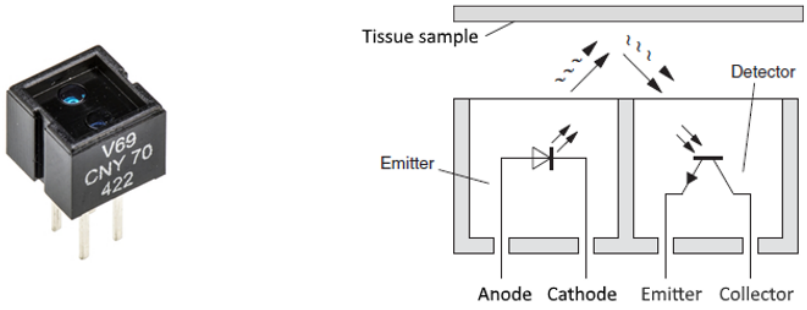

Figure 4.6: CNY70 photocoupler.

4.3.3 Extension sensing element

As the extension sensor, the CNY70 photocoupler was applied (Fig. 4.6). The CNY70 is a reflective optical sensor with a transistor output. For better light reflection, there is a source of light in the CNY70, which is represented by an infrared LED and which emits towards the tissue under investigation. The infrared emitter produce the light with the wavelength of 950 nm. The reflected light is sensed by a phototransistor, which produces an analog electrical signal according the reflected light absorption. The CNY70 has also build-in daylight blocking filter. Its typical applications are optoelectronic scanning, optical switching elements, and other optical sensing devices. However, photocouplers can also be used as galvanic isolation to avoid direct connections of two or more electrical circuits. This is also in our case as well; because the CNY70 photocoupler practically divides the designed hardware into two circuits – the emitter circuit and the detector one. Among the electrical characteristics of the CNY70, it is important to notice the following electrical parameters:

- for the emitter: forward current IF = 50 mA; forward voltage VF = 1,6V;
- for detector: typical output under test IC = 1 mA; maximum collector current IC = 50 mA; peak operating distance is less than 0,5 mm.

As it can be seen from the Figure 4.6, the infrared light produced by the emitter propagates in the cultivation chamber's environment and encounters the tissue sample. At the

medium-tissue boundary, some part of the emitted light is reflected and directed to the detector's side. The detector, phototransistor, sense the light variation and produces the corresponding electrical current on transistor's emitter-collector line - either increasing or decreasing the current in dependence on the absorbed light.

However, there are also several problems occurring when dealing with the optical sensing systems. Firstly, in case of an additional boundary between the tissue sample and the detector, the reflected light may be partly dispersed. This fact can significantly affect the results of the measurements. In our case, it is a sample mounting plate made of transparent silicon and placed in a cultivation chamber. The CNY70 photocoupler has to sense the tissue sample's extension through this plate. Therefore, tests with the silicon material should be done in order to establish the possibility of tissue extension sensing through this material.

Secondly, one of the main obstacles of such a sensing system can be hidden in ambient light. The ambient light can directly influence on the photocoupler's performance and distort the measurements. Although, there is an integrated daylight blocking filter in the CNY70; the tests of the photocoupler in an ambient light's environment are necessary. See the test results in "*Calibration tests*" subchapter.

4.3.4 Other electronic components

As in the case with the pressure sensor electronics, for basic electric circuit design, standard RLC electronic elements – resistors and capacitors of 1206 series were used. Resistors were mainly used as voltage dividers, pull-up resistors, gain setup resistors, and current limiters. Capacitors were introduced into electrical circuit with purpose of power stabilization, noises suppression, and provision of better measuring. For external power supply and input-output signal transmission, WAGO-256 connectors and standard male pin 2.54-mm-spaced headers were used.

LM317 three-terminal adjustable regulator is an adjustable positive-voltage regulator capable of supplying more than 1,5 A over an output-voltage range of 1V25 to 35V (Fig. 4.7a). It requires only two external resistors to set the output voltage. Moreover, the LM317 has an internal short-circuit current limiting system and thermal overload protection. The most typical LM317 applications relate to the field of biometrics, optical networking, spectroscopy, digital signage, infusion pumps, etc. In the extension sensor's hardware design, the LM317 works exceptionally on the emitter side; it serves mainly for the stabile and

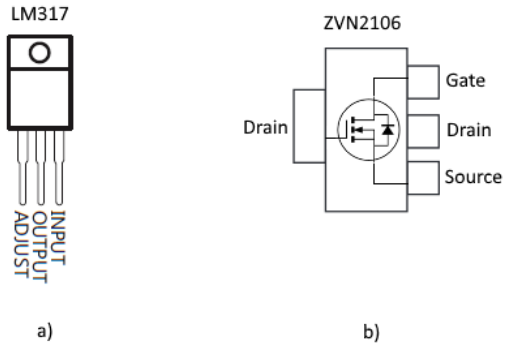

Figure 4.7: Extension sensor's electronic components.

precise power supply and limits the emitter's current. The precise current on the emitter's side and overall stabile power supply in the electrical circuit assures the steady and accurate functioning of the infrared emitter and, hence, stable light emission on the extension tissue. In the extension sensor's design, the LM317 three-terminal regulator is adjusted to 44,4 mA by the 27 Ohm resistor and additional transistor's and emitter's loads. However, by this current value, voltage dropout of the LM217 amounts to around 1,7V. The voltage dropout of the emitter itself is around 2V.That means that, by the initially planned +3V3 voltage power supply, the emitter will lack of voltage. In this situation, the LM317 should be supplied by a higher voltage power supply, namely connected to the cultivation chamber's +5V power supply rail. This will help to avoid the instability of the current in the emitter's electrical circuit.

LM4132 voltage reference is a precision voltage reference (Fig. 4.4a). It is used on the detectors side for stabile and precise power supply of the reflected light detector; hence, for obtaining the steady and accurate informational signal of the tissue sample's extension rate. The LM4132 produces stabile and precise power supply of 2V. However, the voltage reference can produce up to 20 mA current output. It has low temperature coefficient and low supply current – 60 μA. All these parameters are suitable for the extension sensor's detector side and should ensure the optimal and stabilized tissue extension's data acquisition. This electronic component is also used in the pressure sensor design.

ZVN2106 transistor is a N-channel metal-oxide-semiconductor field-effect transistor (N-MOSFET) (Fig. 4.7b). Its functioning is based on the use of electrical field to control the conductivity of a channel with negative type of charge carriers. In our hardware design,

the N-channel MOSFET was used for switching the electric signal of the emitter. As an electronic circuit's element, the main advantage of a MOSFET is that it requires very little current on its Gain pin to get activated and start delivering a much higher current to a Drain-Source load (10 to 50 times or more) (McGowan K., 2012). In the case of ZVN2106, it turns on by 1mA (0,8-2,4V gain-source threshold voltage) and can deliver loads up to 450 mA currents and 60V.

TLC271 operational amplifier is a programmable low-power operational amplifier (Fig. 4.4b). The output of the photocouplers's detector is up to 1V in the ideal reflective material and operating distance less than 0,5mm. So the real signal will be even less. Therefore, after the informational signals from the detector enters the hardware, it should be amplified first. The amplification assures the stronger signal, which can be processed easier and get less influence from the external and inner noises. For this purpose, TLC271 amplifiers are implemented into the extension sensor's hardware design. As an operational amplifier, its gain can be set easily by the ratio of the resistors on its negative feedback line. The exact nominals of the resistors can be set only after the test though. The TLC271 electronics are designed for single-supply operations with a low-noise (high-bias) mode and with common-mode input voltage extending below the negative rail. These characteristics make the TLC271 a suitable operational amplifier for extension signal processing.

ADS1115 analog-to-digital convertor is an ultra-small, low-power, 16-Bit ADC with internal reference (Fig. 4.4d). The ADS1115 has two differential or four single-ended signal inputs, wide supply range from +2V up to +5V5, programmable data rate from 8 up to 860 samples per second (SPS), programmable comparator, and an internal programmable-gain amplifier. The parameters of the ADS1115 are suitable for the extension sensor's signal processing and converting it from analog into the digital one. In the case of the extension sensor, the power supply will be +5V, data rate will be set for default 128 SPS, and PGA will be encoded for the 2x amplification. The PGA setting also declares the full scale – the range of the input voltage, which will be digitalized. The full scale will amount to the value of ±2.048V. However, the input analog signal of the tissues sample's extension measurement will be amplified to the full scale range by an external amplifier TLC271. The address pin, ADDR, will be connected to the GND in order to set the ADS1115's slave address to 7-bit form of 100 1000 binary number. The ADS1115 is also used in the pressure sensor designed; see "Pressure sensor design – ADS1115 analog-to-digital convertor" subchapter for more detailed description.

Most of the ADS1115 parameters are set by the initial communication with an external MCU. For this purpose, there is an output for the I2C electronic bus connection of the ADS1115. There are serial data line (SDA) and serial clock line (SCL) pinouts for I2C bus. In our case it will be used for a communication of the ADS1115 with an external MCU for further data transmission, processing and user-friendly visualization.

4.3.5 Initial setup of the I2C electronic bus

An I2C communication between MCU and ADS1115 in the extension sensor design is similar to the I2C communication in the pressure sensor (See "*Pressure sensor hardware – Initial setup of the I2C electronic bus*" subchapter). Accordingly, the initial address setting of the i2 communication should be:

1. Writing to Config register (setup).

    - the first byte set the ADS1115 address: **0100 1000** in binary form or 0x48 in hexadecimal form , where there are 7 bit of I2C address followed by a low "Read/Write" bit. In our case, the last bit is set to "Write" state.
    - The second byte switches the ADC's Pointer register to the Config register by sending **0000 0001** in binary (0x01 in hexadecimal form) byte and activates it.
    - the third byte and the forth bytes set the ADS1115 Config register parameters, which will ADS working parameters. The third byte is the most significant byte (MSB) of the Config register setup. It should be **1011 0100** in binary form or 0xB4 in decimal form, because:

      - Bit 15 (operational status / single-shot conversion start): 1 - start of a single conversion;

      - Bits 14:12 (input multiplexer configuration): 000 - AINP = AIN0 and AINN = AIN1 (default).

      - Bits 11:9 (programmable gain amplifier configuration): 010 - full scale of ±2.048V (default).

      - Bit 8 (device operating mode): 0 - continuous conversion mode.
    - The third byte is the less significant byte (LSB). It should be **1000 0011** in binary form or 0x83 in decimal form, because:

- Bits 7:5 (data rate): 100 - 128 samples per second (default).
- Bit 4 (comparator mode): 0 - traditional comparator with hysteresis (default).
- Bit 3 (comparator polarity): 0 - active low (default).
- Bit 2 (latching comparator): 0 - non-latching comparator (default).
- Bit 1:0 (comparator queue and disable): 11 - disable comparator (default).

2. Setting the pointer register to conversion mode

   - The first byte is as usual the ADS1115's slave address of **0100 1000** in binary form (0x48 in hexadecimal form) followed by a low "Read/Write" bit.
   - The second byte sets the Pointer register to the Conversion register, which contains the results of last conversion, and activates it by sending the **0000 0000** in binary form (0x00 in hexadecimal form).

3. Reading out the Conversion register.

   - The first byte sets the ADS1115's slave address of **0100 1000** in binary form (0x48 in hexadecimal form) followed by a high "Read/Write" bit.
   - The first incoming byte from the ADS1115's Conversion register is the most significant byte of the last conversion made.
   - The second incoming byte is the most significant byte of the last Conversion made.

These bytes have to be taken into consideration while initializing the microcontroller-ADC communication and obtain the data from the pressure transducer. The received data is than processed either in the MCU or computer.

4.3.6 Power supply unit

The already existing cultivation chamber has a +24V power supply and consequent voltage rail. As it was stated in the "*Extension sensor design*" subchapter, the designed hardware for the tissue extension's sensing requires +5V or +3V3 power supply. Therefore, the special 24V-to-5V transformer was designed and added to the designed hardware for the +5V voltage power supply (See the Appendix D for the electrical circuit diagram). The input of the transformer is attached to the +24V rail of the existing cultivation chamber via the 25 pin connector. The power supply's On/Off modes are controlled with a standard switch button on the designed enclosure box.

4.3.7 Nominals of extension sensor's electronics

According to the electronic component's choice and power supply for the extension sensor's hardware design, there are several RLC electronic elements, which nominals should be calculated and adjusted to provide the adequate hardware functioning and proper extension sensing output. Therefore, according to the set ADC full-scale range of ±2,048V and the single +5V supply operations in the designed hardware, the sensor output after the acquisition and amplification should not exceed the range from 0 to +2,048V on the input of the ADC. With respect to this fact, several resistors' and capacitors' nominals are described below, These RLC elements set the amplification gain and the current for emitting and sensing part of the extension sensor.

According to the CNY70's photocoupler's datasheet, the current in the emitting part, namely by the CNY70's infrared LED was adjusted to the 50 mA by the *R1* resistor. According to the LM317 adjustable regulator, the output current Iout is set by the following equation:

$$R_1 = \frac{1,25V}{I_{out}} = 24\ \Omega \tag{4.3}$$

Furthermore, there is also a ZVN2106 N-MOSFET transistor in the emitting line, which serves as a switch and controls the infrared LED functioning. In order to set the right electrical signal on the gait of the ZVN2106, *R3* and *R4* resistors were added to the hardware design. The R3 =1 kΩ resistor serves for the current limitation while the R4 =10 kΩ serves as a pull-up resistor.

The CNY70's sensing part with a phototransistor is supplied by the LM4132 voltage reference. In this case, a pull-up *R2* resistor was added into the sensing line with a nominal of 1 kΩ.

According to the preliminary calibration tests of the CNY70 photocoupler (See the "Extension sensor testing" subchapter), the maximum sensed output could almost reach 1V, consequently the input of the TLC271 instrumentation amplifier as well. Therefore, as the ADC's input should have not exceeded the range from 0 to +2,048V, the double amplification ($G = 2$) performed by the TLC271 was sufficient. The TLC271 instrumentation amplifier's gain setting is calculated as following:

$$G = 1 + \frac{R_6}{R_5} \tag{4.4}$$

From the equation 4.4 and according to the necessity to provide double amplification, the nominals of the *R5* and *R6* were chosen at the value of 2,2 kΩ.

Moreover, according to the electronics' datasheets, the nominals of the *C1* and *C2* capacitors are chosen with values 10 μF and 1 μF respectively for the better power supply's noise suppression (LM4132 Datasheet, 2016). Similarly, the *C3* capacitor have nominals of 100 nF for more stable power supply of the TLC271 instrumentation amplifiers.

4.4 Software

4.4.1 Pressure signal acquisition and processing

For the obtaining of the pressure SCW Medicath transducer's data, the specific hardware was designed. The hardware obtains precise and accurate pressure value of the medium inside the cultivation chamber in an analog way. Thereafter, the build-in ADS coverts the analog values into digital pressure ones according to the set bitrate. Whereupon, the hardware possesses an SDA and SCL output for the I2C electronic bus communication. However, the hardware itself is not sufficient technique to obtain the desired pressure sensor's values. The pressure signal should be also processed and recalculated to the user-friendly view by a software.

For this purpose, the special software in the ARDUINO programming environment in a object-oriented manner was designed. ARDUINO is a microcontroller-based software and hardware kit for "building digital devices and interactive objects, which can sense and control physical devices" (Wikipedia, 2016). For programming the microcontrollers, there is an integrated development environment, which provides the full coding functionality based on *C* or *C++* programming languages.

The main algorithm of the designed software is represented on the Figure 4.8. According to the pressure sensor's hardware design and the given task of this master thesis, software has to provide a completion of several tasks and requirement. They are as following:

1. Communicate with the external devices via a given protocol (I2C electronic bus) fast and steady;

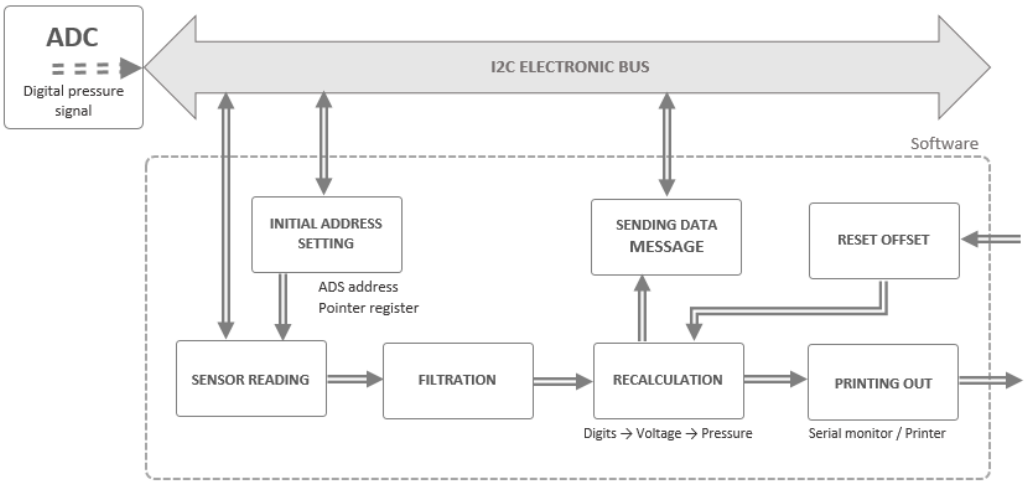

Figure 4.8: Signal processing algorithm. Software level.

2. Receive the data from sensors (hardware) accurately and reliable;
3. Process (perform filtration, computation, scaling, recalculations, etc) the received data accurately;
4. Send ready data for printing out in a user-friendly form;
5. Prepare and send ready data in a given format and via given protocol.

According to the designed software algorithm (Fig.4.8) and the above-stated requirements, there are several main blocks in the ARDUINO pressure signal's processing code. Firstly, there is an external I2C electronic bus, which is connected to the microcontroller-based software and the ADS1115 analog-to-digital convertor, which is built-in in the pressure sensor's hardware. ADS1115 possess the digital values of the pressure signal and is able to transfer them to a master device via the I2C bus by request. The communication including settings and requests are done via byte messages. However, to be able to send the request or even to start a master-slave communication, it is necessary to initialize I2C addresses for the slave device and its inner registers. For this purpose, there is an Initial address setting block in the designed software. It stands for a start of the master-slave communication and transmission of the slave device's address and address of its inner registers – particularly, the address of the ADS1115 by the first sent byte and its inner registers by the following bytes. Although, the ADS1115's inner structure consists of several registers,

namely a pointer register and its division into *Conversion register*, *Config register*, *Lo_thresh* register, and *Hi_tresh* register. The designed system is counted upon the Conversion register. Whereupon, after the sending the ADC address by the first byte, the master device should set the pointer register by sending the second byte and set the inner register to the Conversion register mode by sending the corresponding third byte. Afterwards, the Initial address setting block the conversion register. Moreover, by sending the register addresses and settings, the software also install the desired parameters of the ADS1115 functioning. Among them, there are such parameters, which can be tuned by software, as operational status, input channels selection, programmable gain amplifier setting, data rate, comparator mode, and other settings. The exact ADC and its inner register addresses and settings are given in "*Initial I2C communication setting*" subchapter.

4.4.1.1 Data acquisition and filtration

After the initial settings are done, the next task is the digital pressure data's obtaining from the ADC. For this purpose, the software should be able to send the data request from the ADS1115 via the I2C electronic bus. The general call consist of the command with the corresponding ADC address; after which, the ADC sends 2 bytes of the digital pressure values. The pressure values enter the software in the integer form. The ADC's full scale and bit rate determine the number of digits per input volts. This number is calculated as following:

$$Digital\ pressure\ value = \frac{Pressure\ sensor\ voltage\ [\mathrm{V}] \times 2^{bits}}{Full\ scale\ [\mathrm{V}]} \tag{4.5}$$

After the digital value from the ADC is obtained in the Sensor reading block, the values need to be filtrated. The *Filtration* block stands for the pressure sensor's signal optimization. Although, the pressure sensor itself is supplied by a stable and precise 2,048V power supply, which is also reinforced by few capacitors providing a noise suppression on the hardware level. The precise power supply helps in delivering the steady and accurate pressure values. However, there can be small fluctuations in the pressure sensor's measurements due to the pressure changes itself or minor noises in the electric circuit. In the designed software, these noises are suppressed by simple smoothing the pressure value by calculating its average value. The averaging rate can be set manually in the software.

Another common sensor's problem is so called zero drift – a shift in the whole calibration of the sensor due to slippage or undue warming of the electronic circuits. To eliminate

this problem and reset the zero value, there is a special *Reset offset* block in the designed software. Firstly, the pressure in the cultivation system should be dropped to the normal value of 0 mmHg (atmosphere pressure). This can be done by the revelation of the medium in the system and its opening to atmosphere. Secondly, the *Reset offset* function detects the activation of the external Zeroing button located on the enclosure box, calculates the average zero value corresponding to the provided pressure value, and refresh the value of the pressure sensor's offset in the software. The new value of the offset is than utilized the further calculations as following:

$$\textit{Corrected pressure value}\ [\mathrm{V}] = \textit{Current pressure value}\ [\mathrm{V}] - \textit{Pressure offset}\ [\mathrm{V}] \qquad (4.6)$$

However, it also should be mentioned that the initial value of the pressure offset is set to the value of the common voltage value of 107,6 mV due to the problem of the common voltage in the pressure sensor hardware design (See the "*Common voltage*" subchapter).

4.4.1.2 Recalculation block

The *Recalculation* block stands for converting the digital pressure value, which comes in an ADS's integer output form, into the user-friendly appearance, namely converting into the units of millimeters of mercury (mmHg). However, in order to provide to pressure units, a conversion from digits into the voltage should be performed first.

The ADS1115 is 16 bit analog-to-digital convertor. Its full scale is usually preset by an initial communication with the ADS1115. However, the ADS1115's output is known as a signed integer. That means that one bit is used to indicate if the integer value is positive or negative. This fact leads to conclusion of only 2 $\times$(16-1) = 32768 possible output values to indicate the magnitude of the measurement.

According the ADC's initial settings of the pressure sensor's hardware, the full scale of the ADS1115 amounts to the value of $\pm$2,048 Volts. Consequently, the ADS's digital output of 32767 would represent a value of 2,048 Volts. Hence, according to the formula 4.5, the division of 2,048V by 32767 yields a scale factor of **0,0625 mV** per bit of the implemented ADS1115.

After the conversion of the digital ADC value into the voltage values is completed, the Recalculation block converts the voltage value into the user-friendly pressure value. According the pressure sensor tests, its dependence on the input voltage excitation, linear pressure

dependence, its sensitivity and other characteristics (See the "*Pressure sensor*" subchapter), the pressure value in mmHg can be calculated as following:

$$\textit{Pressure value}\ [\text{mmHg}] = \frac{\textit{Current pressure value}\ [\text{mV}]}{\textit{Sensitivity}\ [\text{mV/mmHg/V}] \times \textit{Voltage excitation}\ [\text{V}]} \tag{4.7}$$

For the pressure sensor's data processing, the pressure sensitivity of 0,005075±0,000036 mV/mmHg/V was used. As for the excitation voltage supply of the pressure transducer, according to the PCB electronic component's choice (See the "*Other PCB electronic components*" subchapter), there is a LM4132 voltage reference for the powering up the pressure transducer. It produces stabile and precise power supply of 2V – the value used in the software calculations.

4.4.1.3 Print-out and data transfer

After the calculations are done, the results in the user-friendly form are transferred further on for the *Printing-out* block, which stands for the results visualization. In ARDUINO software environment, the results are printed in a serial monitor. In other conditions, they can be transmitted to a printer or a display.

However, after the *Recalculation* block, the results can also proceed to the *Sending Data Message* block. The block stands for transferring the filtrated and calculated pressure values as a data message to an external device, which can be another computer, software, MCU, etc. The pressure data is transformed to bytes and transferred via the I2C port. The message itself is coded by the binary synchronous communication (BSC) protocol. BSC is "an IBM character-oriented, half-duplex link protocol" (Wikipedia, 2016) using only three characters for encoding the text message. According to the BSC, all messages are framed into so called single framing, where ¡STX¿ byte (hexadecimal code 0x02) stands for a start of the message; and ¡ETX¿ byte (hexadecimal code 0x03) stands for an end of the message. Because the message send in the byte form, the pressure data is transformed into the integers first, than encoded in the form of two 8-bit words (most significant byte and less significant byte consequently). The final byte attached to the data message is so called longitudinal redundancy check (LRC) byte. LRC is an analog of the checksum data, which stands for the detecting errors during data transmission or storage. After the data message is complete, it is finally written to the serial I2C electronic bus so that an external device could read it out.

The software itself stands for the pressure sensor's data processing and corresponds to all given requirements as data acquisition, data processing, and data transmitting. The full ARDUINO code for the pressure sensor's data processing is given in the Appendix F.

4.4.2 Extension signal acquisition and processing

Mainly, the extension signal acquisition and processing on the software level is equal to the pressure signal acquisition, processing and further transmission. On the hardware level, an initial setting of the ADC parameters is different. The setting bytes are described in the "*Extension sensor design - Initial setup of the I2C electronic bus*" subchapter).

All the function blocks of the extension sensor's algorithm are similar to those on Figure 4.8 except the Recalculation block. In this block, the extension sensor's voltage is converted to the tissue extension value according to the calibration curves of the CNY70 photocoupler (See "*Extension sensor calibration*" subchapter).

After the recalculation, the extension value is also transmitted further on via the Bisync protocol in similar way as the pressure signal.

4.5 Mechanical construction

4.5.1 Holder modification of the cultivation chamber

These chambers provide both the living conditions and the mechanical stress that is necessary for developing aortic valve tissue. All parts of the dynamic cultivation system, which are in contact with cultivation media, tissues and living cells are made from non-toxic materials, e.g. aluminum, silicone, santoprene, or similar. All of these materials are suitable for sterilization with an autoclave or other chemical and radiation sterilization, which minimizes the risk of contamination during some long-term experiments.

However, according to the designed pressure and tissue extension's sensors, some changes in the cultivation chamber design should have been introduced to fit in the sensors. Mainly, sensor holders were needed.

The pressure transducer itself has no need on the special solid holding or attachment part as long as it is connected to the medium system and peristaltic pump flow accordingly by silicon tubes. Although, the extension sensor required special holder for an attachment of the

CNY70 photocoupler to the cultivation plate. Cultivation plate itself, where the cultivation ring with a sample tissue is installed, did not undergo any changes in the design. The 3D sketches of the holders, cultivation chamber plate and complete assembly's construction was done in the Inventor CAD software. The designs of these elements are given in the Appendix G.

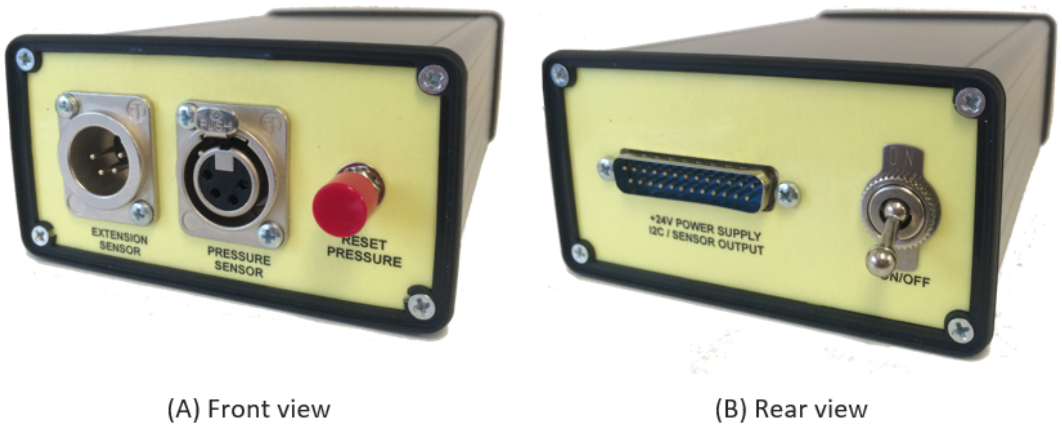

Figure 4.9: The final appearance of the designed device.

4.5.2 Enclosure and connectors

An enclosure and outfit of the device for supporting the pressure and tissue extension sensing is also of high significance. The proper enclosure provides the sealed boxed for the safe and stable functioning of the designed hardware. For the hardware instalment and its functioning, an aluminum enclosure of Hammond Manufacturing was utilized. The dimensions are as following: length 160 mm, width 103 mm, height 53 mm. See the Appendix H for a detailed technical documentation.

The pressure and tissue extension sensors are attached to the cultivation chamber and connected to the enclosure with separate 4-wires cables. For the sensor cable's connections, standard 4-pin DLX connectors from the Neutrik company were used.

For a connecting the device to an external receiver for data transfer via I2C-protocol and power supply, a 25-pin connector is used for input-output communication. Moreover, the connector also includes separate pins for the pressure reset function, extension sensor's

switch control, and analog outputs of the pressure and tissue extension sensors. See the Appendix H for a detailed pin description of this connector.

As for other additions to the enclosure panels, two buttons were added. One push-button on the front panel is used for the *Reset* function (See "*Pressure signal acquisition and processing*" subchapter) of the pressure sensor. Another switch-button was used for powering up 24V-to-5V transformer and the whole designed hardware system consequently.

The final appearance of the device with an enclosure, buttons and connectors could be seen on the Figure 4.9.

4.6 Pressure calibration method

The selected *SCW Medicath* Disposable Pressure transducer implementation had to pass several test before its implementation into the system and signal processing. The test were performed in order to prove the linear dependency of the pressure transducer's response, its dependence from the input voltage excitation, dependence from the inner medium, as well as calibration and sensitivity of the pressure measurements. During the tests, the random two pressure transducers were selected out of several dozens. The pressure was tested within two mediums: air and liquid (water). The pressure itself was produced by a precise pressure delivery machine. The power supply of the pressure transducer amounted to different values from +1V up to +10V supply on Excitation+ pin and GND on Excitation- pin. The output signal was measured from the Out+ pin in correspondence to the Out- pin. The results of the calibration experiments of the pressure transducer can be found in the "*Results - Pressure sensor testing*" subchapter.

4.7 Extension sensor calibration method

As it was previously mentioned in the "*Extension sensor*" subchapter, the optical sensing method was chosen because it provides non-touch measurements to the sealed and sterile inner environment of the cultivation chamber with a pericardium sample and living cells in it. More specifically, the method of a light reflection was used in the created device. As a sensing element, the CNY70 photocoupler have been take. For better light reflection, there is a source of light in the CNY70, which is represented by an infrared LED and which emits towards the tissue under investigation. The reflected light is sensed by a phototransistor,

which produces an analog electrical signal according the reflected light absorption. The light is reflected from the diaphragm, where the seeded pericardium is installed. The intensity of the reflected light, and the sensor's output voltage consequently, is dependent on the distance between the diaphragm and the base line of the CNY70's phototransistor. Hence, the value of the diaphragm extension and consequently pericardium extension can be calculated from the phototransistor voltage output. However, a calibration of the extension sensor for the designed cultivation chamber should be done. Therefore, the relationship between the sensor's output and the distance from the CNY70's sensing part to the pericardium sample, which will be extended under the pressure applied, should be investigated. For this purpose, a special testing module from the designed CNY70 holder was derived (Fig. 4.10).

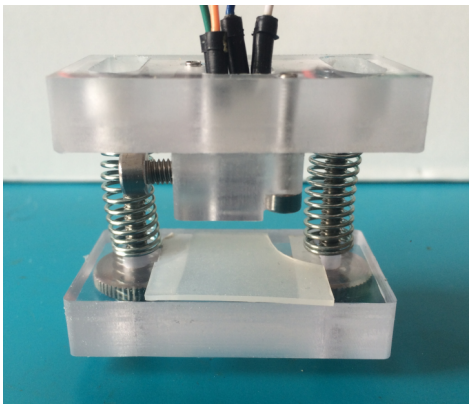

Figure 4.10: Testing module for the extension sensor preliminary calibration.

The module consisted of two main parts. The first one – the upper part was used to be the same CNY70 holder designed for the cultivation chamber. The second part – the lower one was designed especially for the calibration tests with adjustable distance to the upper part. It was determined to mount sample materials, which were tested, on it. The lower part has basically represented a plate with double screws and a holder for a sample material. The complete testing module was 3D-printed from the polycarbonate material.

There were two types of calibration tests:

- Type I: dependence of the sensor's output signal to the material under investigation and distance from the material to the CNY70's phototransistor.
- Type II: dependence of the sensor's output signal to cultivation chamber's diaphragm extension according to the pressure delivered.

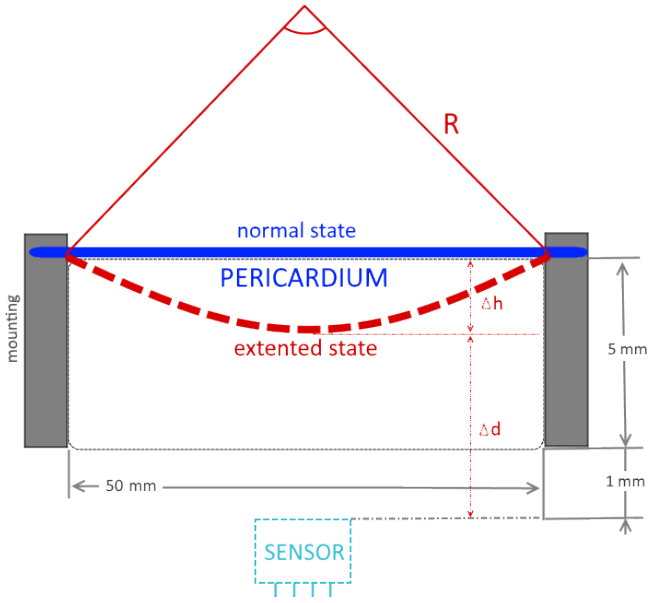

Figure 4.11: Diaphragm extension's calibration method.

If the idea of Type I calibration is clear, the idea behind the Type II calibration should be described. The Figure 4.11 represents the main theory of calibration calculation of the diaphragm extension dependent on the distance to it. According to the standard practice of the arc length calculation, the following formulas were used:

$$R = \frac{h}{2} + \frac{c^2}{8 \times h} \tag{4.8}$$

$$\alpha = 2 \times arcsin \frac{c}{2 \times R} \tag{4.9}$$

where Δd - distance from the sensor to the diaphragm; Δh - the height of the diaphragm extension; R - radius of the extended diaphragm; α - angle of the extended diaphragm; L - length of the diaphragm, ΔL - relative extension of the diaphragm. In this case, the diaphragm extension is calculated as following:

$$L = \alpha \times R \tag{4.10}$$

However, the main goal behind this calculations is to find correlation of the relative extension of diaphragm and the sensor output.

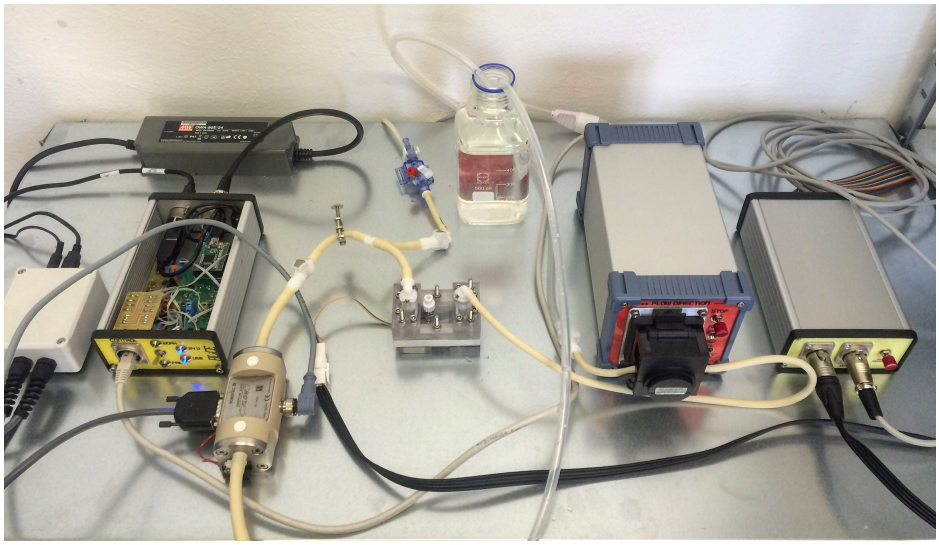

Figure 4.12: Operating cultivation system for diaphragm extension calibration.

In the above-stated cases, the created testing module was used only in the first type of experiments. In the second type of experiments, the pericardium sample was investigated in the real designed cultivation chamber in order to establish the real values of diaphragm extension. The complete cultivation system for diaphragm extension calibration with the working pressure and extension sensors can be seen on the Figure 4.12.

The results of the calibration experiments of the extension sensor can be found in the "*Results - Extension sensor calibration*" subchapter.

4.8 Ambient light exclusion

The CNY70 photocoupler is a light sensitive element, which output voltage is dependent on the amount of light, exposed to the CNY70's phototransistor. In case of the CNY70 photocoupler, light comes mostly as the reflectance from a built-in infrared LED. However, there is also a light, coming from the outer environment, called ambient light.

The testing measurements with ambient light were taken around midday with a slight daylight, with room lights off. The distance to the sample material was 10 mm. As it can be seen on Figure 4.13, the phototransistor possesses some noises and fluctuations in dark conditions. The ambient light produces even more fluctuations in the CNY70's sensing output.

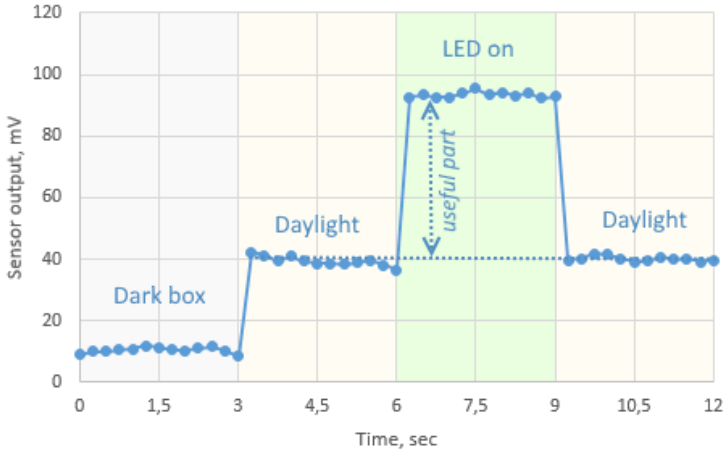

Figure 4.13: Ambient light detection.

To avoid this problem, there is a solution by creating a sensing pulsation. According to this solution, there is a switch button on the designed hardware to create a sensing pulsation. While the switch button is in an off-mode, the CNY70 photocoupler senses the ambient light. When we turn on the CNY70's infrared LED, there is an increase in the sensor's output due to the reflected light. As the switch button goes shortly in an on-mode, the photocoupler starts sensings the ambient light plus the CNY70's emitter reflected light. The useful signal from those two signals is easily derived by introduction of a high-pass filter and by an subsequent subtraction of two signals on software level giving us the real value of the light reflected from a CNY70's emitter.

4.9 Perfusion flow modulation

According to the utilized idea of pressure delivery by medium flow in the cultivation chamber, the peristaltic pump, generating this perfusion flow, had to be also calibrated and set up for the different modes of operating pressure and flow rate. General structure of the flow calibration setup is shown on the Figure 4.14.

For the medium flow generation the *WMC* peristaltic pump has been chosen. According to the design of the peristaltic pump, medium movements inside a perfusion system are produced by positive displacements of spring rollers. The speed of the peristaltic pump is usually directly affecting the flow. Number of the spring rollers, on its turn, is generally

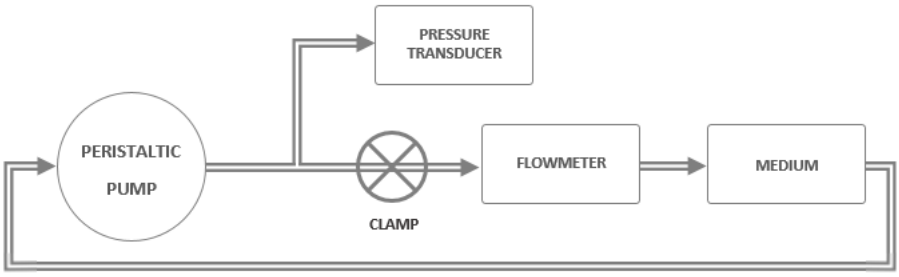

Figure 4.14: Structure of perfusion flow modulation's tests.

affecting the form and the frequency of the flow waves. In order to prove these theory, the flow modulations with *WMC* peristaltic pump rotors, possessing from 2 up to 6 spring rollers, were conducted. The speed of the rotor was also tunable.

However, the flow can be also altered by the radius of the tubing used in the peristaltic pump, especially in the part, affected by the spring rollers. In that concern, for an additional flow modulation testing, different types of tubings were also utilized. In the tests, four types of flexible plastic *PharMed Saint-Gobain* tubings, installed in the spring roller setup, were used. Namely, there were tubings with inner (outer) radius of 1,6 mm (4,8mm); 3,2 mm (6,4 mm); 4,8 mm (8,0 mm); and 6,4 mm (9,6 mm).

During the tests, pressure values were continuously measured. In order to purposely affect the operating pressure and to alter its value, a clamp was introduces into the testing structure.

As a test fluid, the normal tap water was used. The medium flow was measured by the *Sonoflow IL 52/3* flowmeter from *SONOTEC* company. The results of the flow modulation tests can be found in the "*Results - Flow modulation calibration*" subchapter.

4.10 Differentiation method

The differentiation of the adipose derived stem cells (ASC) and endothelial cells (HUVEC or HSVEC) into a prosthetic aortic valve tissue will be carried out in the modified cultivation chamber with the designed pressure and tissue extension sensors. The sensor data is dedicated to let the differentiation procedure be more informative and improve its biological properties. However, except the technical aspects of the cultivation chamber, biochemical properties of the differentiation technique should be also mentioned.

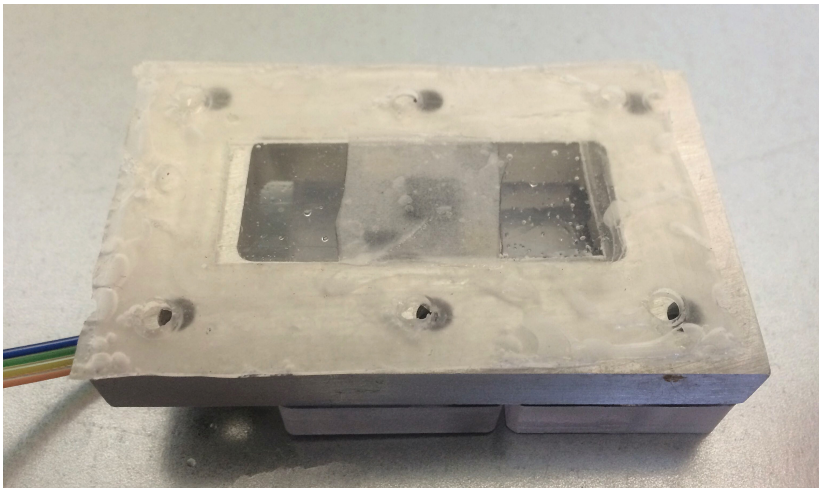

Figure 4.15: Decellularized and cut pericardium sample prepared for installation into cultivation chamber.

4.10.1 Pericardium sampling

For growing an aortic valve prosthesis, autologous or allogenic samples of bovine, porcine, or human decellularized pericardium were used, seeded with human ASCs and covered by human endothelial cells (Ghodsizad A. et al., 2014). In experiment, conducted in this master thesis, the pericardium, harvested from pigs after euthanasia, was used. Preparing a pericardium sample usually involves also the process of pericardium decellularization and chemical cross-linking (Filova E., 2014).

On the Figure 4.15, a sample of decellularized pericardium, used during extension sensor's calibrations tests, can be seen. It is placed on diaphragm of the cultivation plate, right before mounting the upper part of the cultivation chamber and starting the tissue extension tests.

4.10.2 Applied differentiation technique

Endothelial and other cells adhere weakly to the non-modified pericardium. Therefore, the inner and outer layer of the pericardium sample is firstly covered with a layer of fibrin gel. The technique involves a growing a fibrin network from a substrate surface, which let the cell's ingrowth while coating the surface of pores. Moreover, the thickness of the fibrin network is adjusted so that the "cells could migrate and proliferate in the decellularized pericardium sample" (Filova E., 2014). The cells themselves are not impaired due to usage of

biomolecules, which are participating in normal regeneration processes of a damaged tissue. The fibrin coating includes fibronectin and laminin, which significantly improve the adhesion and proliferation of the ASCs. The fibrin coating also includes extracellular-matrix-proteins and growth factors (like epidermal growth factor (EGF), fibroblast growth factor-2 (FGF-2) and vascular endothelial growth factor (VEGF)), which have to attract cells into pores and stimulate their proliferation. These biomolecules have to encourage recellularisation and endothelialization of the pericardium sample. Additional mechanical load in various directions is applied in order to the whole sample would proliferate cells, build up the extracellular matrix, synthetize collagen, and remodel the tissue into aortic valve interstitial cells or smooth muscle cells. Finally, the recellularized pericardium has to be endothelialized by endothelial cells and covered with second layer of the fibrin-fibronectin coating. The complete cultivation procedure in a cultivation chamber takes 3-4 weeks. Afterwards, the artificially grown aortic valve prosthesis is tested for its mechanical characteristics, stem cells differentiation rate, ECM formation and endothelialization rates (Filova E., 2014).

4.10.3 Biological and mechanical evaluation

For a verification of the correct applied differentiation technique, as well as for the designed pressure and extension sensor's prove testing for correctness of construction and application, there should be biological and mechanical evaluation of the cultivation system and pericardium tissue in it during or after the conducted experiments. In this case, it is necessary to select appropriate evaluation techniques and methods.

As for the biological evaluation, it will not be taken into consideration in this master thesis will be done by biologists at the IoP Academy of Science of the Czech Republic. However, it should be said that an identification and quantitative analysis of ECM proteins, namely their growth and proliferation will be processed by the method of mass spectrometry. For the analysis of the pericardium samples, their decellularied and recellularized states, as well as the native pericardium tissue – all exposed to the cyclic strain stress and cultivation media will be analyzed. This analysis will be mainly conducted by estimation of the protein content – Type I collagen, Type III collagen, and elastin. Fibrous collagen structures will be visualized by multi-photon microscopy using a second harmony generation technique (Filova E., 2014).

For evaluation of the biomechanical parameters of the tissue, the most interesting and important are the mechanical parameters of the recellularized pericardium, which should provide information of the grown aortic valve prosthesis suitability for an aortic valve replacement procedure. The material stiffness is characterized firstly by the Young's modulus (tensile and elastic). It is also known as the elastic modulus and characterizes mechanical property of linear elastic solid materials (Hibbeler R., 2013). The formula of the Young's modulus is defined as a relationship between stress δ and strain ε in a material and calculated as following:

$$E = \frac{\delta}{\varepsilon} \tag{4.11}$$

The stress δ is defined as force F per unit area A, which is actually nothing else as the pressure. In this calculations, we could use the pressure P from the pressure sensing system. The strain ε is defined as a proportional deformation of the material ΔL to its original size L. In our case, it is deformation of the pericardium sample inside the cultivation chamber, which is sensed by the tissue extension's sensing system. Therefore, the formula of the Young's modulus could be rewritten in the following form:

$$E = \frac{F/A}{\Delta L/L} = \frac{P}{\Delta L/L} \tag{4.12}$$

Concluding the above-stated, it has to be mentioned that the higher the Young's modulus in the case of the pericardium extension, the more rigid is the pericardium sample and the more collagenous structure the cells have produced. This could be a representative variable of the momentary biomechanical property of the pericardium sample during the experiments.

Tensile and elastic parameters are crucial for the proper functioning of the aortic valve prosthesis after transplantation. "Measurements of the pressure drop over time provide information about leaflets closing tightness and suitability of replacement" (Filova E., 2014). A big advantage of this sensor system is that it can provide continuous measuring during the experiments and enable to find trends on environmental conditions, which the pericardium tissues under investigation are put into. However, these results calculated derived from the sensor's data will not be the best option of exact results how stiff or tensile pericardium sample is. For exact comparison and for a statistical evaluation, tensile tests will be performed using a universal tensile testing machine.

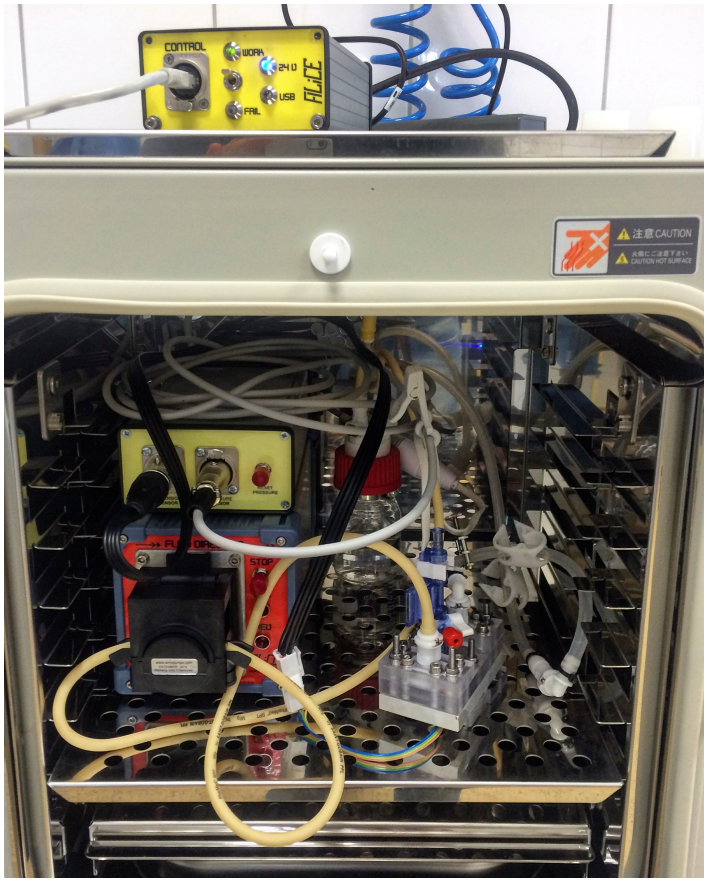

Figure 4.16: Complete cultivation system in the thermal box during single experiment on living cells.

4.11 Experiment overview

The complete set of the cultivation system is represented on Figure 4.16. It was placed in the thermal box in order to maintain the normal human temperature of 37°C. A planar pericardium structure was used for the single experiment. The pericardium sample with the fibrin-fibronectin coatings was placed in a modified cultivation chamber. During the laboratory experiment, an integrated peristaltic pump was producing defined force and mechanical stress inside the bioreactor medium, applying it to the pericardium sample. The peristaltic pump's function was controlled with the measured pressure as a feedback variable. For mounting a modified pericardium tissue inside the cultivation chamber, there was an elastic silicone ring. The silicon ring is usually melted specially for this purpose in a specified geometrical shape, which allows the pericardium structure deform under the strain stress to defined values.

The experiment was taken in two scenarios. The first scenario was to determine the non-toxicity and suitability of system for ASC and endothelial cells. The second one was held on decellularized pericardium tissue in order to determine the collagen production.

Chapter 5

Results

5.1 Pressure sensor testing

During the SCW Medicath Disposable Pressure transducer implementation, several test with the pressure transducer were conducted. The test were performed on order to prove the linear dependency of the pressure transducer's response, its dependence from the input voltage excitation, dependence from the inner medium, as well as calibration and sensitivity of the pressure measurements. During the tests, the random two pressure transducers were selected out of several dozens. The pressure was tested within two mediums: air and liquid (water). The pressure itself was produced by a precise pressure delivery machine. The results of the pressure transducer's test with the voltage supply +2V on Excitation+ pin and GND on Excitation- pin are given in the Table 4. The Out+ voltage values given in the table were done by measuring the voltage on the Out+ pin in correspondence to the Out- pin. As the result of the pressure transducer test with +2V power supply, the linear dependence of the sensor response was proved. One of the measurements are visualized on Figure 5.1a. Moreover, the average sensitivity of the pressure transducer by +2V power supply was found out, which amounted to the 0,5034 ± 0,0097 mV per each 50 mmHg. From these values, it was also assumed the general sensitivity of the pressure transducer in relation of ΔOut+ / Pressure / Excitation+, which amounted to 0,005034 ± 0,000097 mV / mmHg / V. In order to control the dependence of the pressure sensor output to the input voltage power supply on the Excitation+ and Excitation- pins, the additional tests with +1V, +2V5, +5V, and +10V power supply were conducted. Further more, these test were also conducted to confirm the calculated sensitivity value of the pressure transducer. The results were similar

Table 5.1: Pressure sensor tests with +2V power supply.

Ex+	2	V
I	0,822	mA

*averaged for both sensors

**averaged for both sensors for air and liquid medium

Pressure, mmgH	Sensor 1 Out+, mV		Sensor 2 Out+, mV		Δ Out+, mV*			Δ Out+ / Pressure / Ex+, mV/mmHg/V
	Air	Liquid	Air	Liquid	Air	Liquid	Average**	
0	0,0223	0,0307	0,0221	0,0407				
50	0,5263	0,5795	0,5140	0,5714	0,4979	0,5395	0,5179	0,005179
100	1,0283	1,0994	1,0186	1,0607	0,5033	0,5042	0,5038	0,005038
150	1,5439	1,5718	1,5113	1,5514	0,5039	0,4813	0,4923	0,004923
200	2,0634	2,0770	2,0040	2,0420	0,5057	0,4978	0,5018	0,005018
250	2,6008	2,5959	2,5018	2,5332	0,5168	0,5047	0,5107	0,005107
300	3,1123	3,0734	2,9996	3,0244	0,5046	0,4843	0,4942	0,004942
					Average		0,5034	**0,005034**
					±		0,0097	0,000097

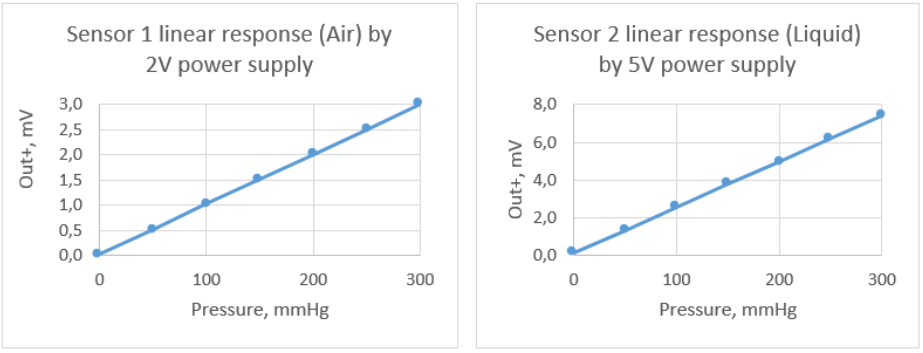

a) *b)*

Figure 5.1: Pressure sensor response.

Table 5.2: Pressure sensor tests with +5V power supply.

Ex+	5	V
I	2,045	mA

*averaged for both sensors

**averaged for both sensors for air and liquid medium

Pressure, mmgH	Sensor 1 Out+, mV		Sensor 2 Out+, mV		Δ Out+, mV*			Δ Out+ / Pressure / Ex+, mV/mmHg/V
	Air	Liquid	Air	Liquid	Air	Liquid	Average**	
0	0,1299	0,0307	0,1102	0,1552				
50	1,3396	1,3566	1,3402	1,3050	1,2198	1,2316	1,2256	0,004903
100	2,5792	2,6657	2,5795	2,5634	1,2394	1,2832	1,2610	0,005044
150	3,8021	3,7845	3,8098	3,7744	1,2266	1,1630	1,1940	0,004776
200	5,0250	5,0408	5,0401	4,9854	1,2266	1,2333	1,2299	0,004920
250	6,2435	6,4330	6,2752	6,1948	1,2267	1,2944	1,2596	0,005039
300	7,4620	7,5951	7,5102	7,4041	1,2267	1,1853	1,2056	0,004823
					Average		1,2293	**0,004917**
					±		0,0274	0,000109

to the +2V power supply. There were linear responses of the pressure values. A random pressure transducer input-output dependence is given on Figure 5.1b; however, the pressure transducer output was proportionally increased or decreased to the input voltage supply on the Excitation+ pin. On Figure 5.2, the overall dependence of an input voltage supply to the pressure transducer output is shown. As it can be seen, the pressure sensor has also linear response to the power supply. This fact gives a variety of voltage power supply's options; however, as it will be stated below, the precise voltage reference of 2V will be used in the hardware design for the pressure transducer power supply. The measurement differences between two randomly chosen pressure transducers were about 0,36% , which proves the interchangeability of the sensors. After all the test measurements with different voltage power supplies, the average sensitivity amounted to **0,005075 ± 0,000036 mV/mmHg/V** (millivolts per 1 mmHg of pressure per 1 Volt of power supply). The standard deviation was 0,7%. These values will be used further on in the software design and encoded into the signal processing scripts.

5.2 Flow modulation tests

As it was mentioned in the "*Methods - Perfusion flow modulation*" subchapter, the medium flow produces the pressure inside the cultivation chamber and effects on the living cells,

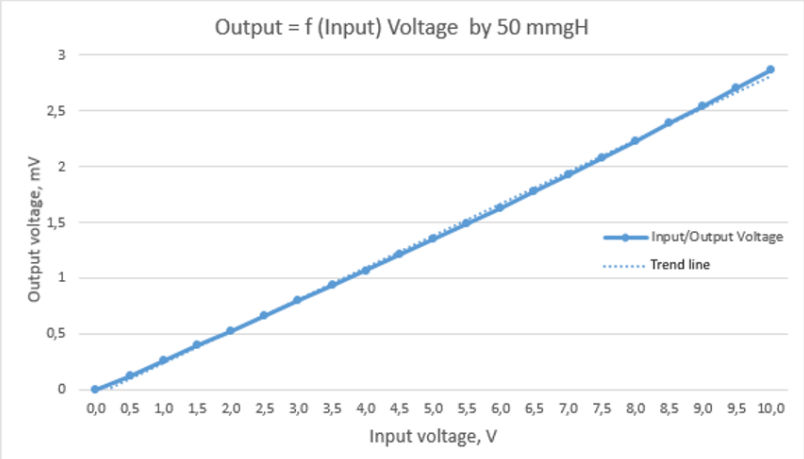

Figure 5.2: Pressure sensor input-output dependence.

seeded on the recellularized pericardium tissue. The medium flow is created by a *WMC* peristaltic pump. Mainly, the following parameters of the cultivation system can vary from the peristaltic pump settings:

- speed and waveform of the medium flow (ml/min);
- value and waveform of the operating pressure (mmHg);

However, many settings of the peristaltic pump could affect the above-stated parameters. Changes in the following settings were tested:

- diameter of the tubings, installed the spring roller module (mm);
- speed of the peristaltic pump (revolutions/min);
- clamp addition to the flow system.

An uncontrolled altering of these parameters could lead to the undesirable consequences in real experiments.

5.2.1 Dependence on tubing diameter

While moving spring rollers, the peristaltic pump provides the movement of the medium placed inside a tubing. In this case, the diameter of the tubing, installed in the peristaltic

Table 5.3: Flow and pressure dependence on tubing diameter (peristaltic pump with 6 spring rollers, 1 revolution/min)

Tubing diameter, mm	Flow, ml/min	Pressure, mmHg	Flow*, ml/min	Pressure*, mmHg
1,6	8,75	6,6	8,31	158,4
3,2	26,37	8,4	25,73	139,5
4,8	50,12	5,8	48,17	147,6
6,4	61,80	22,5	58,50	210,1

pump motor, directly affects the volume of the medium, which is pushed by a movement of a single spring roller. Theoretically, the more the diameter of the tubing, the more volume of the medium fluid should be moved; consequently, the higher the medium flow should be.

The results of practical experiments are represented in the Table 5.3. In this experiment, peristaltic pump with 6 spring rollers was utilized. Its speed was set up on 1 revolution per minute for all types of tubings. Moreover, the experiments were also conducted in the conditions without and with adding a clamp to the medium flow system in order to investigate clamp effect on the flow changes. The values with the clamp adding are signed by * in the table.

As it can be seen from the Table 5.3, there is a direct dependence of the tubing diameter and the flow, namely, the increase of the tubing diameter causes the increase in the flow rate. Maximum flow rate by speed of 1 revolution per minute amounted to 61,80 ml/min. As for the same experiments with the clamp, there is no significant differences in the flow values. This means that the clamp adding does not play role in the flow rate changes, at least in the created conditions.

As for the pressure changes, in normal conditions without the clamp, there is an average value of the pressure around 5-8 mmHg. However, by the higher rates of the medium flow, it has reached the value of 22,5 mmHg. Moreover, the clamp adding also alters the pressure values. During the experiments, the pressure values up to 400 mmHg could be obtained by the clamp compression ratio.

Talking about the waveforms, it should be mentioned that tubing diameters also effect the waveforms of the flow and pressure rates, delivered into the cultivation system. Visualisation

of the waveforms during the experiments with different tubing diameters are represented on Figure 5.3. The speed was constantly set at the value of 1 revolution per minute.

As it can be seen form the Figure 5.3, during normal medium flow, namely, without adding any clamp, there are pretty strong oscillations in the flow rate. However, by increasing the tubing diameter, the oscillations are decreasing. Moreover, the oscillations can be also diminished by adding a clamp. As it can be seen from the right part of the Figure, the flow oscillations significantly decreasing; however, the pressure value rises abruptly. In addition, the changes in pressure value have high amplitude, which makes an obstacle in providing a stable pressure value. Only in case of the 6,4 mm tubing diameter, the pressure value has rather low amplitude.

5.2.2 Dependence on peristaltic pump speed

The rotation of the peristaltic pump's motor is set by a inner stepper, which, on its turn, set the string rollers speed. In the conducted experiments, the speed of the peristaltic pump's motor was ranging from 0 up to 4 revolutions per minute. The experiments were done in two different variations - with and without a clamp adding. The tubing with 3,2 mm diameter was used in both cases. The results of the experiments carried out are shown on the Figure 5.4. The results of the experiments provide an important insight into the peristaltic pump linear dependence between the flow rate and the peristaltic pump speed, namely, revolutions per minute of its spring rollers. Furthermore, by adding a clumo into the system, it was proven that the flow rate got a variation around $\pm$7,61% - the precision, which is determined to be in order for the following experiments on living cells.

5.2.3 Dependence on number of spring rollers

The rotation of the peristaltic pump's spring rollers provides the movement of the medium. Although, the flow is set only by the speed of the peristaltic motor but by number if the spring rollers, rotating in this motor per unit of time. During experiments, two peristaltic pumps with 3 and 6 spring rollers were tested. Both of them were tested in the same speed of 1,5 revolutions per minute and with the same tubing of 3,2 mm diameter.

Results of the pressure experiments are represented on the Figure 5.5. As it can be seen, peristaltic motor with 6 spring rollers provides more oscillations on the pressure value

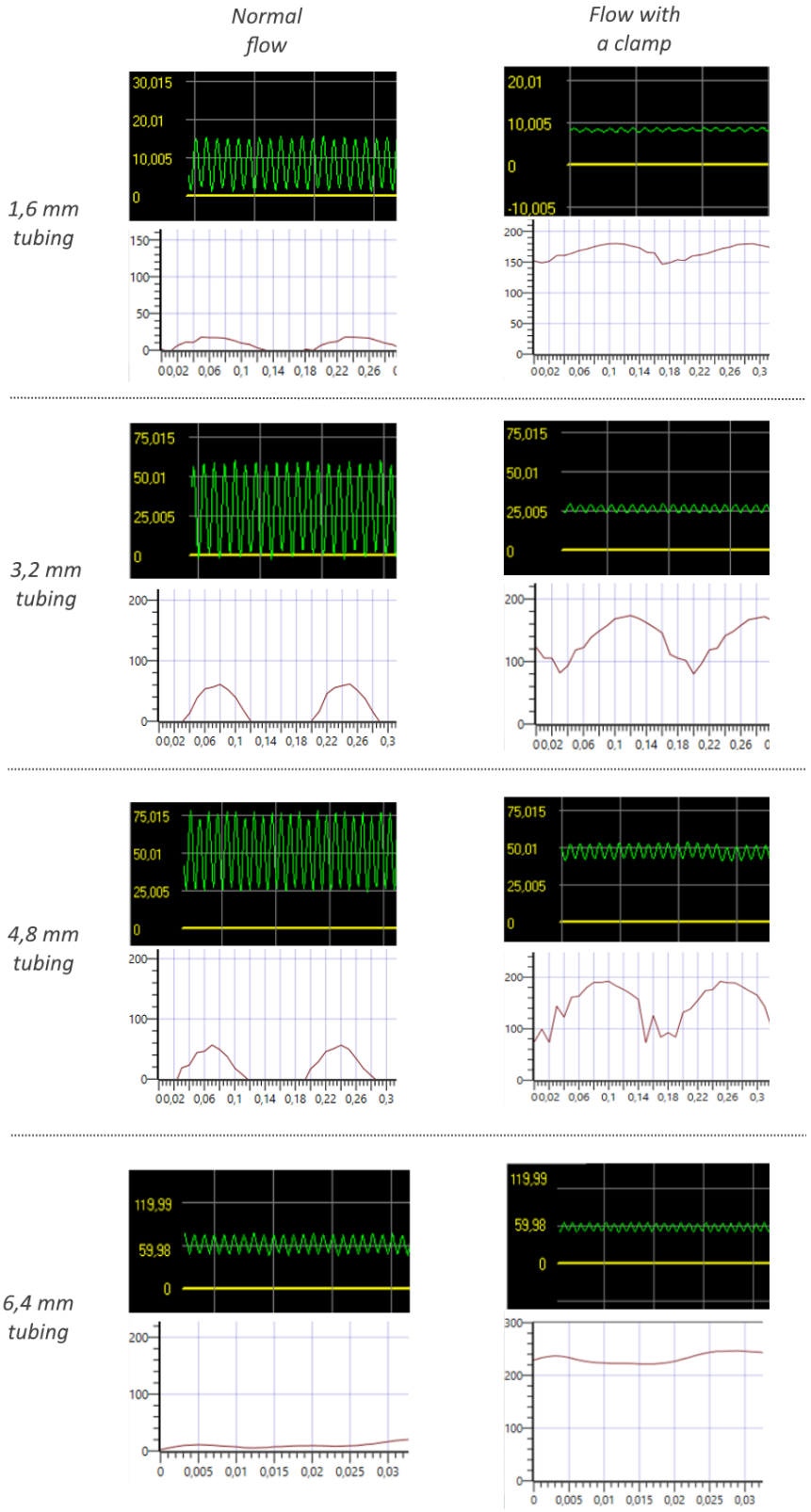

Figure 5.3: Flow and pressure dependence on tubing diameter with and without a clamp by 1 revolution/min.

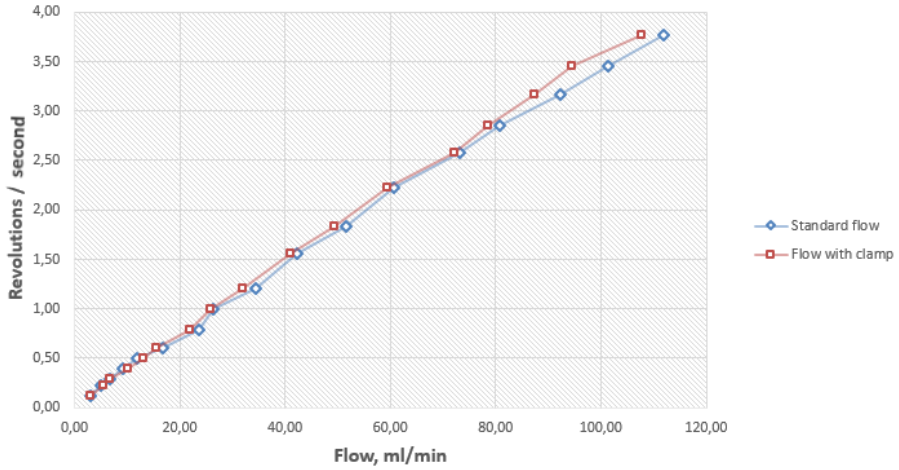

Figure 5.4: Flow dependence on the peristaltic pump speed with 3,2 mm tubing.

during its functioning. By adding a clamp, the pressure values are increasing; but nevertheless, amplitude of the fluctuations rise as well. Although, it is worth of admitting, that the 3-spring-roller motor provides pressure fluctuations of lower amplitude and much lower frequency.

Results of the flow experiments are represented on the Figure 5.6. In opposite to the pressure values, the 6-spring-roller motor produces less fluctuations in the flow values in comparison to the 3-spring-roller motor. However, the clamp improves the situation with the flow fluctuations, there are still some of them, especially in the case of 6-spring-roller motor. And another trade-off for the fluctuations decrease is a rise of the pressure value. However, it should be mentioned that the 3-spring-roller motor provides the sinus flow variations of lower frequency. That is due to the two times less number of spring rollers. But that means also that the frequency of the flow and pressure values can be varied by the number of spring rollers, namely from 0 up to (4 rotations per second * 6 spring rollers) = **24 Hz**.

5.3 Extension sensor calibration

5.3.1 Type I: Material calibration tests

In order to establish the best suitable material of the cultivation chamber and its diaphragm production, test with the extension sensor on different materials were conducted. It was important because the diaphragm material, where the recellularized pericardium which will

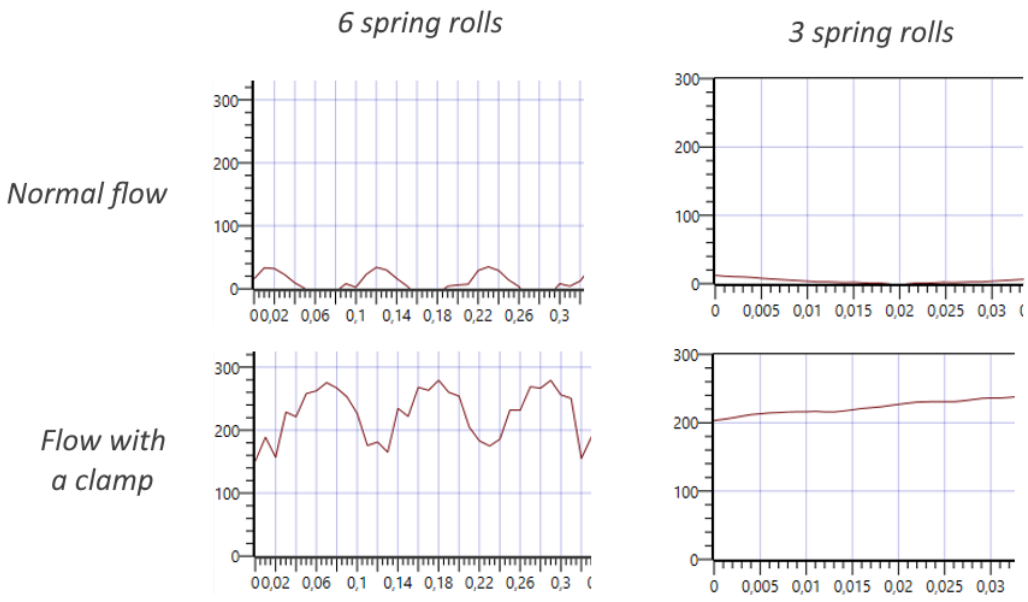

Figure 5.5: Medium flow with and without clamp in a peristaltic pump with 3 versus 6 spring rollers.

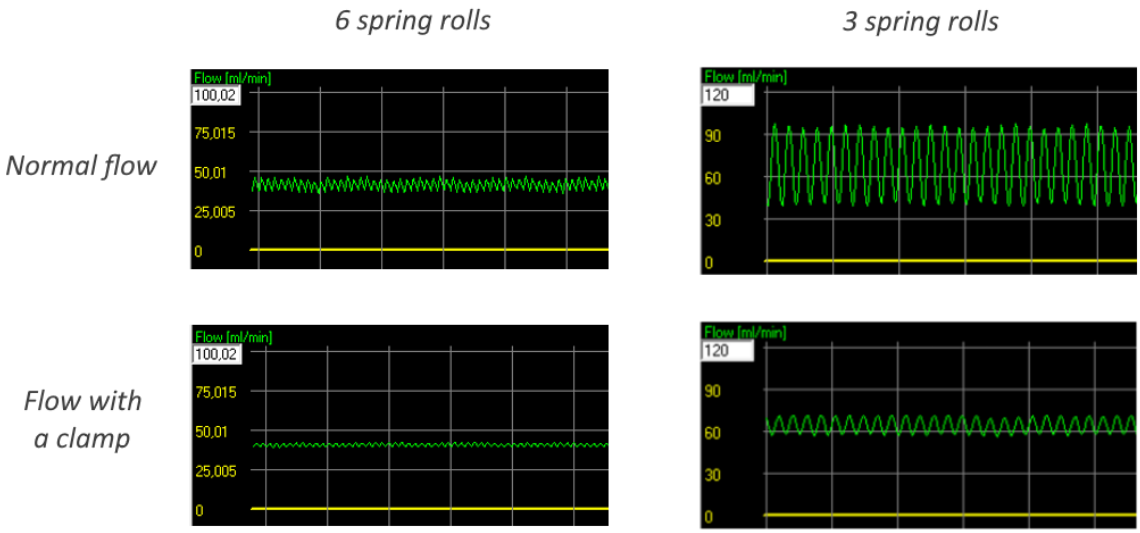

Figure 5.6: Pressure values with and without clamp in a peristaltic pump with 3 versus 6 spring rollers by 1,5 revolution/min in a 3,2 mm tubing.

be extended under the given pressure, has to be the primary source of the tissue extension data.

Among tested materials, there were a simple polycarbonate surface, white sticker, white and black glue band, semi-transparent and non-transparent silicon, cultivation ring material (a derivation from silicon). All these materials either are used or could be used in the cultivation chamber design. The measurements were carried out during the day with a slight

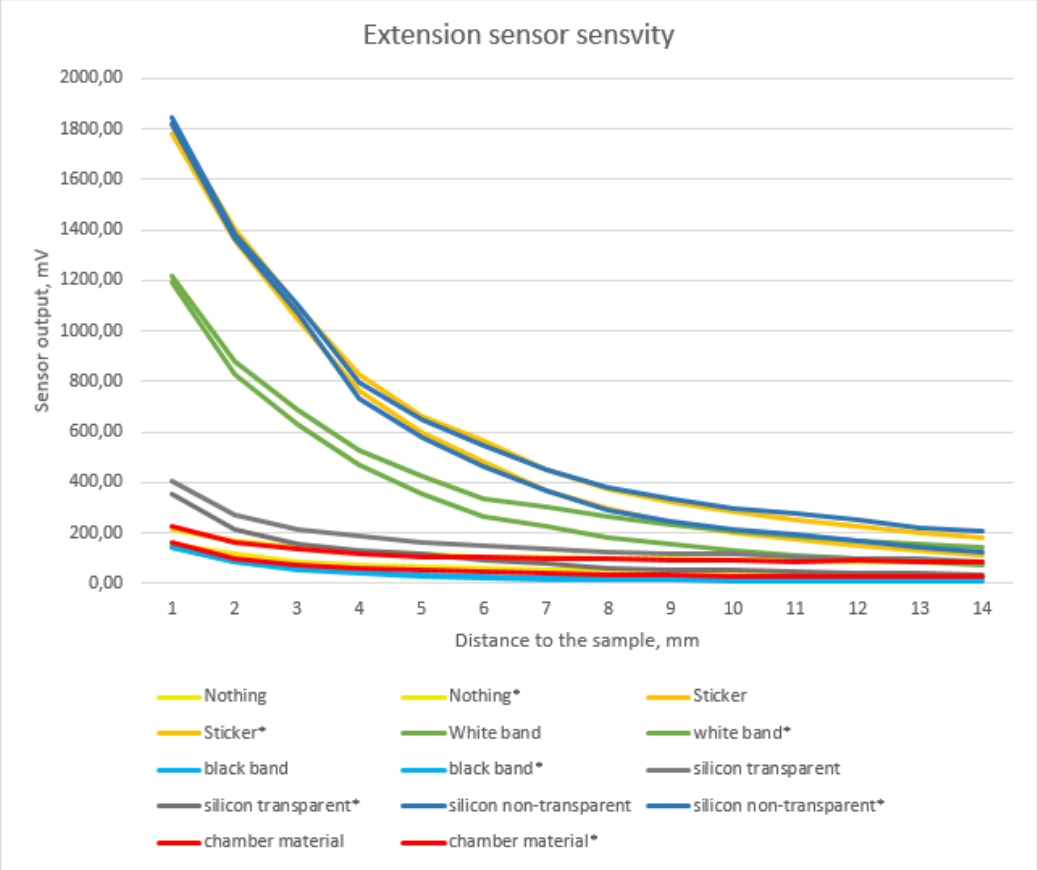

Figure 5.7: Pressure sensor input-output dependence.

daylight from the outside with room lights off. The distance between the sample material and the baseline of the CNY70's phototransistor varied from 0 to 14 mm. Materials were mounted in the specially designed testing module (Fig. 4.10) (See the "*Methods - Extension sensor calibration*" subchapter).

However, the light sensing elements, like the CNY70 photocoupler, are always affected by the environmental conditions, namely by an ambient light. The ambient light makes

an offset in the sensor output measurements; therefore, additional tests in complete dark conditions were conducted. For this purpose, the testing module with a sample material was placed in a dark box. These results of the test without ambient light are signed by * sign on the Figure 5.7. All sensor values are given after hardware amplification.

As it can be seen from the Figure 5.7, there are different non-linear responses for different types of materials. The highest responses were obtained for the white sticker and non-transparent silicon, which is also more close to be of white color. The maximum sensor output reached up to 1800 mV, what was close to the ADC maximum of 2,048 V. These high values were obtained due to the white and glance-like surface of the materials. The next best result was obtained by white band. The maximum output voltage amounted to 1200 mV. However, the most interesting material in our case was chamber material for a chamber ring, which is used in real experiments and where the living cells are placed during cultivation process. The sensitivity for the material was not too high and reached the value of around 220 mV by 1 mm distance to the phototransistor. This calibration curve was not enough sensitive to make the measurements in real experiments. However, the other materials were also not taken into consideration due to their lower extension and stretch properties, which could badly affect the pericardium extension during cultivation under operating pressure.

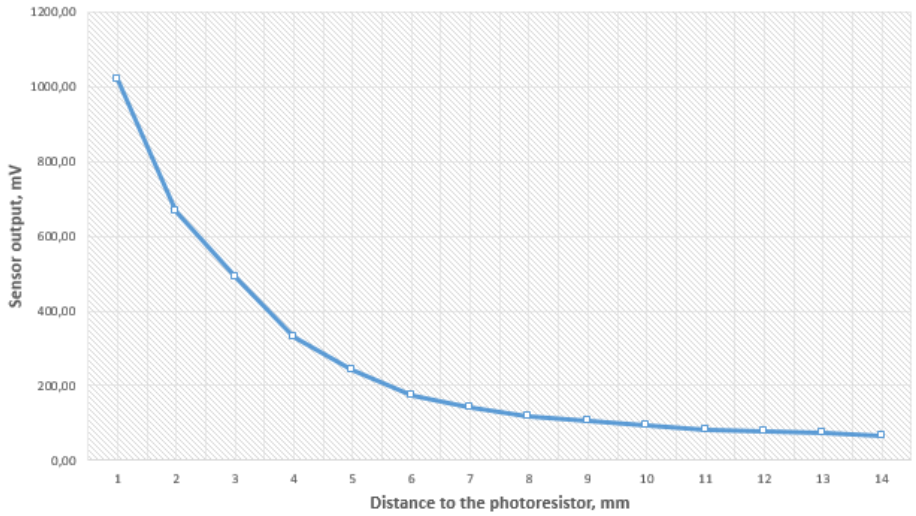

Figure 5.8: Extension sensor's calibration curve.

In this case, the solution was found in increasing the reflectance rate of the chamber material by putting a colored spot on the place of the extension measuring. Namely, a

Table 5.4: Extension sensor's calibration values

Distance, mm	1	2	3	4	5	6
Sensor output, mV	1019,41	664,9	488,95	329,14	241,19	175,63
Distance, mm	7	8	9	10	11	12
Sensor output, mV	143,38	119,07	105,25	92,44	82,44	78,88

spot was put by a blue marker from on the outer surface of the cultivation ring, where the CNY70's infrared LED was pointed. According to the introduced **reflectance spot**, the calibration curve with a higher sensitivity has been obtained (Fig. 5.8).

As it can be seen from the Table 5.4, the output reached the values up to 1100 mV, which was about 5 times more sensitive as before. That values was taken as main calibration curve for experiment measurements, giving an opportunity for even more close measurements with less than 1 mm distance from cultivation diaphragm to the prototransistor.

5.3.2 Type II: Extension calibration in the cultivation chamber

In the previous subchapter, the calibration curve for the CNY70 photocoupler was established according to the silicon material, which was used to production of a cultivation ring and diaphragm. During cultivation process, a pericardium sample is placed on this diaphragm. Although, the calibration curve was obtained; it does not provide us information about the diaphragm and consequently a pericardium sample extension. The calibration curve provides us distance to the diaphragm. Therefore, additional calibration of the sensor output to the diaphragm extension via the calibration curve was necessary.

The Table 5.5 represents the measured and calculated values of the diaphragm extension, where Δd - distance from the sensor to the diaphragm; Δh - the height of the diaphragm extension, L - length of the diaphragm, ΔL - relative extension of the diaphragm. The values were calculated according to the Formulas 6.1, 4.9, 4.10.

According to the obtained values, the complete calibration curve of the diaphragm extension dependent on the sensor output was derived (Figure 5.9). Moreover, as it was implied from the applied methods, the given calibration curve is simultaneously serves as the calibration curve for the pericardium sample extension, because of its tight mounting on the cultivation diaphragm. However, precision of 1 mm looks rough.

Table 5.5: Calibration values of the diaphragm extension

Δd, mm	Δh, mm	Output, mV	L, mm	ΔL, %
6	0	175,63	50,00	0,00 %
5	1	241,19	50,05	0,10%
4	2	329,14	50,21	0,42%
3	3	488,95	50,48	0,96%
2	4	664,90	50,85	1,70%
1	5	1019,41	51,32	2,64%

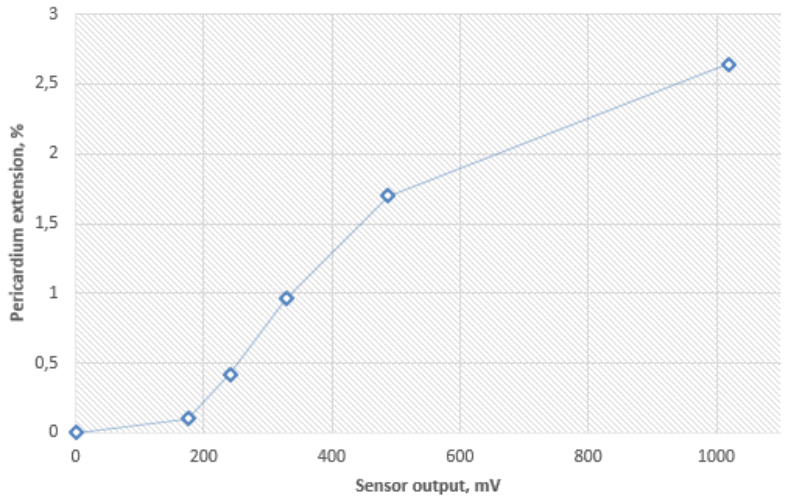

Figure 5.9: Calibration curve of the pericardium sample's extension on the cultivation diaphragm.

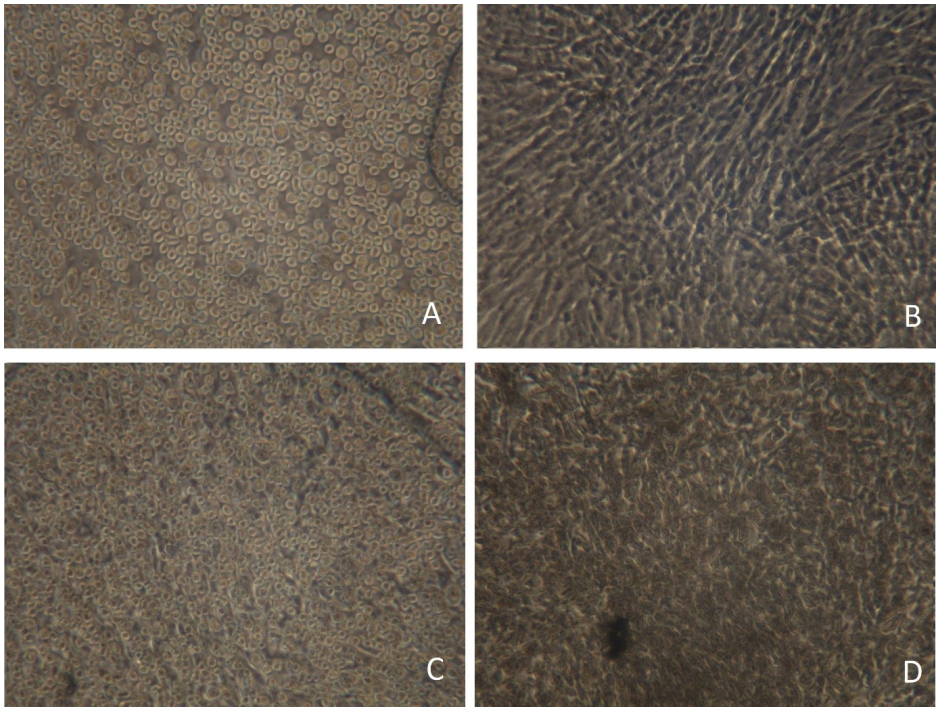

Figure 5.10: Cultivated cells. A – ASC cells after seeding, B – ASC cells in flow and pressure stimulation, C – added HUVEC cells and D – co-culture in dynamic stimulation.

5.4 Cultivation experiment on pericardium

After all calibration procedures of the pressure and extension sensors, a single cultivation experiment on pericardium was conducted. Complete cultivation system within a thermal box during the single experiment on living cells is represented on Figure 4.16

The dynamic cultivation of living cells was held in two scenarios. The **first scenario** was to determine the nontoxicity and suitability of system for ASCs and ECs. The diaphragm was coated with collagen type I (from rat tails) and the cultivation system was completely assembled. First the ASCs cells were seeded into system. After initial 1 hour adhesion a small flow was applied (2,5 $\frac{dynes}{cm^2}$ with approx. 0,5% prolongation of diaphragm). With this setup, the cells were cultivated for 24 hours. After the initial time, the HUVEC cells were added to this culture. The co-culture of the HUVECs covered the ASCs was cultivated for next 2 days. The stimulation was raised to 17,5 $\frac{dynes}{cm^2}$ with approx. 2% stimulation. In fig 5.10 are documented native cells.

The second cultivation scenario was held on decellularized pericardium tissue. This tissue was harvested from pigs and was decellularized with SDS and DNAse solution. This tissue was cut to approx. 2,5 cm x 2,5 cm square and also coated with Collagen Type I.

After assembling the system, the HUVEC cells were seeded. After initial phase of adhesion, the pressure stimulation was set to approximately 2% of prolongation. The cells were dynamically cultivated for 40 hours. A static cultivation was also held for comparison along with the dynamic cultivation. After the static cultivations, the pericardium sample with cells were removed and immunohistologically stained for Phaloidin and Collagen type IV (Fig. 5.11).

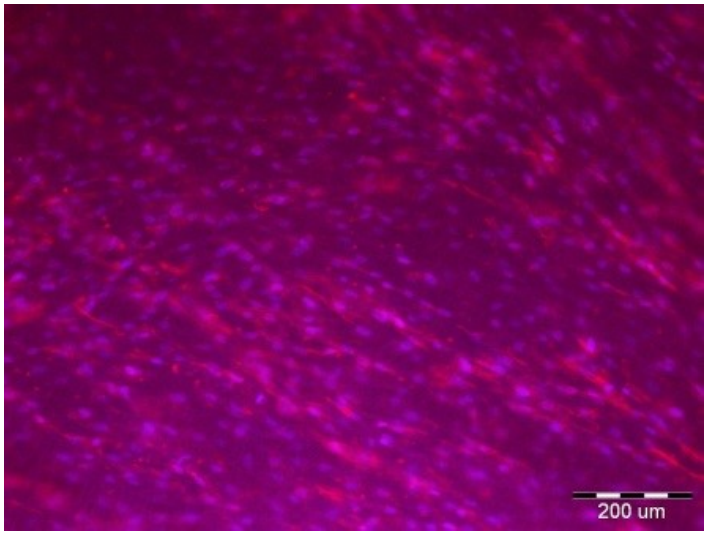

Figure 5.11: The stained pericardium tissue with cells after cultivation.

Collagen Type IV is essential part in aortic valve prostheses development. After the cultivation experiment, the pericardium tissue under investigation, was analysed for the Collagen Type IV production under mechanical stress. As the analyses have shown, there was a significant increase of production of Collagen Type IV in the dynamic cultivation (Fig.5.11(B)) versus the static cultivation (Fig.5.11(A)).

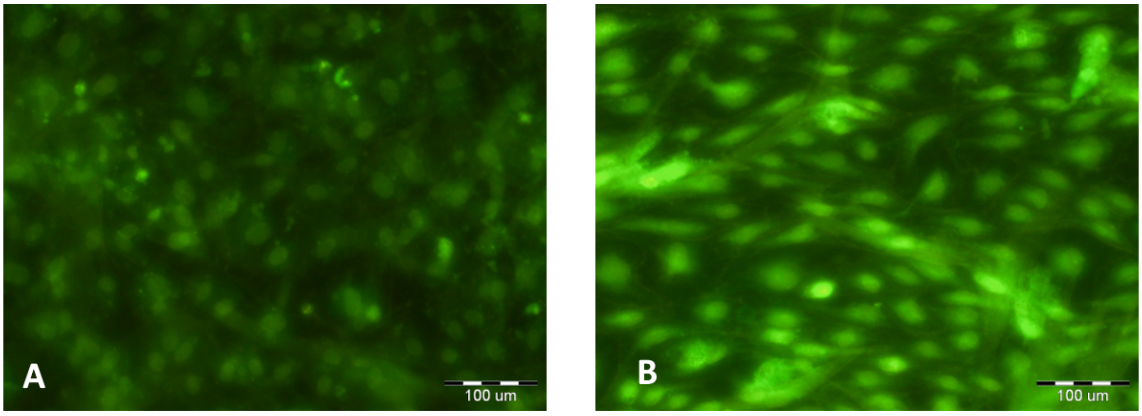

Figure 5.12: Static (A) vs dynamic (B) cultivation of cells. Collagen Type IV marking.

Chapter 6

Discussion

Looking back on the work done in this master thesis, a significant work for improvement of the aortic valve tissue's cultivation technique was conducted. Now, the cultivation chamber (bioreactor), which is used in the IoP Czech Academy of Science, is equipped with a pressure and tissue extension sensor. The sensors were based on the SCW Medicath pressure transducer for the pressure sensor and on the CNY70 photocoupler for the tissue extension sensor.

A big advantage of this sensor system is that it can provide continuous measuring during the experiments and enable to find trends on environmental conditions, which the pericardium tissues under investigation are put into. However there are still some drawbacks in the system; in the following subchapters, they will be discussed more precisely.

6.1 Perfusion flow

During the experiments, an external peristaltic pump was producing flow of the cultivation medium, which was applied in form of mechanical stress to the pericardium sample further on. During the calibration experiments, standard tap water was used as a medium liquid. In the real experiments, the real cultivation medium is also water-based and should not have significantly different density properties, so that it could affect the calibration.

The other points of the perfusion flow settings are discussed below.

Flow rate

As it was shown on the Figure 5.4, the flow rate [ml/min] is linearly dependant on the speed of the peristaltic motor [revolutions/second]. The higher the number of rotations of the peristaltic pump, which is set by an inner electronic stepper, the higher the flow rate.

According to the conducted experiments, the tubing diameter, placed in the peristaltic motor and affected by the spring rollers, influences the flow rate. The Table 5.3 shows the increase of the flow rate with the increase of the tubing diameter. Apparently, the higher tubing diameter provides a bigger volume of the medium liquid during a single push movement of a peristaltic spring roller. There is a direct increase of flow rate by increase of the tubing diameter; although, no linear dependence has been found so far.

Moreover, there is one more factor, influencing on the flow rate. The number of spring rollers, installed into the peristaltic pump's motor, can affect the volume of the medium liquid, pushed through the tubing during a single revolution. As the experiments showed (Fig. 5.5), the higher is the number of the spring rollers, the higher is the flow rate. Furthermore, the flow rate is increasing proportionally to the number of spring rollers.

In that concern, it can be concluded that the flow rate in the cultivation system is a function of three variable:

$$Flow = F\ (Speed\ [revolutions/sec],\ Number\ of\ rollers,\ Tubing\ diameter\ [mm]) \quad (6.1)$$

According to the above-stated parameters, the flow rate in the cultivation system was able to be varied from **0** up to **200** ml/min during conducted experiments.

Flow frequency and waveforms

During the calibration experiments in the laboratory, the flow. The flow forms can be easily seen on the Figure 5.3. They are mostly of a sinus shape with some fluctuations, caused by the electrical ad mechanical noises. The frequency of the flow's sinus waveform is determined by the number of the spring rollers, installed in the peristaltic motor, and its speed in revolutions per second.

Despite the flow modulation in different frequencies, the main idea of the flow provision is that it could be continuously stable and constant. In some cases, the oscillations wre significantly high (See the next subchapter). In addition, flow oscillations cause oscillations

in pressure signal as well. In that concern, the absolute stability of the flow rate could not be reached during the conducted experiments.

It should be mentioned that the 3-spring-roller motor provides the sinus flow variations of lower frequency the 6-spring-roller. That happens due to the two times less number of spring rollers. Although,

All in all, during the experiments, the frequency of the flow values was able to be varied by the number of spring rollers and the peristaltic motor speed. Namely, the sinus form flow frequency could be adjusted from 0 up to (4 rotations per second $\times$ 6 spring rollers) = **24 Hz**. By further motor speed modifications and number of spring roller in the peristaltic motor, the frequency range can be easily enlarged. Although, that might unlikely cause the extreme increase in the pressure values of the inner medium.

As for the other waveforms of the perfusion flow, there was not any. This possibility to provide some other flow waveforms except sinus waves can be done in further investigations.

Flow amplitude and clamp usage

In cases of 3,2 mm and 4,8 mm tubings and by 3 spring-roller-motor, the amplitude of the flow oscillations was significant. In extreme cases, the oscillations amounted to $\pm$154,3% from the average delivered flow rate. Clamp adding usually decrease the amplitude of the oscillations and stabilize the flow wave. In case of 3,2 mm tubing, the amplitude was decreased up to the range of $\pm$4,2% from the average value by adding the clamp. However, a trade-off for the oscillations decrease is a rise of the pressure value.

Regarding the oscillations of the perfusion flow, there were also pressure oscillations in the medium system. By adding the clamp, the average values of the pressure oscillations were even rising significantly up to the 400 mHg. Therefore, the usage of clamp should be strictly controlled and precisely tuned. Another option would be to find a solution so that the pressure and the flow rates could be stabilized independently.

6.2 Pressure sensor

Overall, the pressure sensor was working properly and it was delivering stable signal. However, there is always room for improvement in the stability and precision in signal processing. There still minor uncertainties in the useful pressure signal due to the medium fluctuations,

possible air bubbles in the system and general noise affection. Although, this drawbacks could be improved by an adding couple more pressure sensors into the system (as it was planned from the very beginning) in order to read out the data from different points of the cultivation chamber and perform an averaging.

As for the pressure values themselves, there are still high pulsations in case of 3,2 mm and 4,8 mm tubings. Although, these value pulsations are introduced by the flow inhomogeneity and should be solved mainly by providing a stable flow rate. As well as the forms of pressure pulsations.

6.3 Extension sensor

As for the extension sensor, it was delivering signal, enough stable for the experiments. The extension signal was consequently recalculated into the diaphragm extension value by the obtained calibration curves. The sensor was able to provide continuous measuring during the experiments. Although, several improvements of the techniques could be made.

Calibration curve

It was implied, that the extension of the diaphragm is equal to the pericardium tissue, mounted on this diaphragm. That meant that extension of the pericardium sample was calculated via the calibration curves of the diaphragm extension. Calibration curves are non-linear. they were taken with a step of 1 mm distance from the material under investigation. Especially for software level, it is necessary to enhance the precision of calibration curves, to improve its resolutions and describe the dependence mathematically.

Diaphragm

The tissue extension system is now based on the sensing the diaphragm movement. There are still some fluctuations in the sensing signal due to the small values of the sensed signal and micro-movements of the diaphragm, which is difficult to read out precisely on that micro-level. The better precision of the sensed diaphragm movement should be a primary goal for further improvements in extension signal sensing.

Material

Another point to discuss is material, which the cultivation ring and the diaphragm is made of. During material calibration, the highest sensor output values were obtained due to the white and glance-like surface of the materials. The maximum output voltage amounted to 1800 mV. However, the ADC maximum is 2,048 V and can be scaled even higher. In this case, the further researches should consider idea of taking another non-toxic material with a higher reflectance coefficient for the cultivation ring and diaphragm production. The material with a higher reflectance coefficient could provide more sensitive results of the pericardium sample extension.

Ambient light and other noises

An influence of ambient was successfully suppressed by adding the switching button for making extension sensing pulsations and high-pass-filtering in combination with a signal subtraction on a software level. However, the ambient light filtering system can be further improved in order to set even better sensing precision. As well as the general noise reduction; because even by putting the CNY70 photocoupler in a dark environment with the infrared LED off; the sensing phototransistor produces small noises on the output. In that concern, noise suppression on the sensing part could be and should be improved further on.

6.4 Cultivation experiments on pericardium

The conducted experiment verified that the modified cultivation system is suitable for dynamic cultivation with pressure stimulation and shear stress. The system was nontoxic and provided desired stimulation rate.

The experiment has shown a a significant increase of production of Collagen Type IV in the dynamic cultivation versus the static cultivation, what was one of the main aims of the designed device. As for the pressure sensor, the photocoupler sensed the infrared light reflected from the diaphragm with a pericardium sample in a cultivation chamber. The extension sensor was also working properly. An online sensing provided information about settings and allowed partial adjusting over time.

The results from this cultivation experiment should provide necessary data for optimizing the sensor's system, perfusion system and cultivation bioreactor in general for further

cultivating a pericardium-based aortic valve, especially from tubular pericardium structures. However, for providing more significant results, like production of collagen and elastin, the best conditions for ASC and edothelial cells differentiation, etc., a long term cultivation experiments must be set (at least 3 to 4 weeks).

Young's modulus

Tensile and elastic parameters are crucial for the proper functioning of the aortic valve prosthesis after transplantation. Therefore, the artificial aortic tissue, grown from a pericardium sample in the cultivation chamber, should have been also tested on the tensile and elastic parameters. As it was described in the *"Biological and mechanical evaluation"* subchapter, the correlation between a medium flow and the provided pressure in the cultivation system, namely the *Young's modulus* should have been obtained during the experiments.

However, due to the lack of time and technical inability to record the pressure and extension values continuously over a long period of time, the correlation between the pressure and extension values was not found. The single experiment on living cells took 40 hours with preset values of the tissue extension and operating pressure. However, this correlations and Young's modulus could be and should be investigated in further researches.

6.5 Further modifications and researches

As the further improvement of the designed system, a dynamic cultivation bioreactor of decellularized pericardium could contain several types of additional transducers and sensors, i.e. flow, temperature sensing, conductivity, pH, pO2 and other necessary parameters for maintaining stable living conditions.

Moreover, this was a cultivation chamber for the *planar* pericardium structures. In further researches, the design of the cultivation bioreactor for 3D *tubular* pericardium structures should be done. For that purpose, the cultivation chamber could be modified to grow up a 3D tissue prosthesis within an artificial aorta for the aortic valve replacement by applying a mechanical loading. For example, an elastic silicone polymer could set a defined shape of the artificial aorta and tubular pericardium sample could be than fixed inside the artificial aorta. However, in these conditions, the pressure stimulation also has to be modified. For example, the perfusion rate could provide two types of pressure. The first flow will serve for

opening and closing the artificial aortic valve and the second one will provide the necessary pressure stress, and consequently appropriate physical stimulation, in between for the pericardium sample. The mechanical stimulation as in the case with cultivation of the planar pericardium sample, should encourage the differentiation of the adipose derived stem cells and increase the production of extracellular matrix. These processes improve the mechanical properties of the aortic valve prosthesis constructed from pericardium sample during the aortic valve replacement. However, the pressure stimulation and overall monitoring of a tubular 3D pericardium structure should be more complex; therefore, there is a number of obstacle the further researcher should do as evaluation of mechanical parameters (pressure, valve tightness), control of biological parameters on the whole 3D pericardium surface, tissue extension measuring, etc.

Chapter 7

Conclusion

This master thesis was aiming to improve the existing cultivation system for growing a tissue, which could serve as a living aortic valve prosthesis for further transplantation during a valve replacement surgeries. Flat decellularized samples of pericardium, reseeded with adipose derived stem cells (ASC) and endothelial cells (HUVEC or HSVEC) was considered as the main scaffold for cultivation of aortic valve prosthesis. In order to improve the ASC and endothelial cells differentiation into a living valve tissue, existing cultivation (perfusion) chamber was optimized.

According to the given task, the following tasks were accomplishmed:

- The mechanical and electrical design of cultivation (perfusion) chamber used for was optimized. The special parts for mounting of additional sensing elements (pressure sensor and tissue extension sensor) were designed and produced for experiments. Non-toxic materials, like silicon and polycarbonade, were used for the mechanical construction of the parts, which were in direct contact with the cultivation chamber.

- As long as mechanical load played the decisive role in the aortic valve cultivation, the system for pressure stimulation of recellularized pericardium in chamber including process monitoring instrumentation was designed. Pressure transducer was able to produce output values in range from 0 to +2,048V, calibrated from 0 to 300 mmHg and further transmitted to a 16-bit ADC. The pressure changes within the cultivation system was produced by medium flow and could adjusted from 0 to 300 mmHg by a clamp in the cultivation low system. Medium flow was provided by an external peristaltic pump. By setting up the tubing diameters, number of spring rollers, peristaltic

motor speed, the medium flow could be adjusted by from 0 to 24 Hz pulse waves of different amplitude with an average flow value up to 200 ml/min.

- An optical method, allowing extension sensing of recellularized pericardium diaphragm, fixed in chamber during the dynamic cultivation, was implemented in the cultivation chamber. The extension sensing method was based on detecting the light, emitted from an infrared LED and reflected from the cultivation diaphragm surface. The diaphragm carried the pericardium sample and was able to extent to certain values under operating pressure. Technically, the extension sensor was based on a CNY70 photocoupler. The tissue extension sensor was able to deliver voltage output from 0 to +2,048V and was calibrated to sense extension values from 0 to 14 mm. By calibration experiment in a cultivation chamber, the sensing values of the pericardium sample's extension were set in range of 0 up to 2,64% of prolongation.

- During an experiment of the designed cultivation (perfusion) chamber on real pericardium, a dynamic cultivation with controlled pressure stimulation and tissue extension were conducted. Results of cultivation in designed system were verified and compared with static cultivated culture on decellularized pericardium. The system was proved to be nontoxic and to provide desired stimulation rate. Moreover, the cultivation system has shown a significant increase of production of Collagen Type IV which is essential part in aortic valve prostheses development. For providing more significant results, like production of collagen and elastin, investigating proper values of pressure and flow rates, long term cultivation experiments must be set (at least 3 to 4 weeks).

Overall, the huge work to improve the cultivation system of an aortic valve prosthesis was done. Although, there is still a great space for further optimizations of the cultivation chamber; these accomplishments are devoted to provide better functioning of the cultivation chamber and improved differentiation technique for the aortic valve prosthesis, which, on its turn, has to lead to a better aortic valve treatment.

References

Akins C.W., Buckley M.J., Daggett W.M. Risk of reoperative valve replacement for failed mitral and aortic bioprostheses. Ann Thorac Surg. 1998: 65(6):1545-51; discussion 1551-2.

Alberts B., et al. Molecular biology of the cell, 5th edition. Garland Science. 2008;1726. ISBN9 78-0-8153-4r05.

Balachandran K., et al. An ex vivo study of the biological properties of porcine aortic valves in response to circumferential cyclic stretch. Ann. Biomed. Eng. 2006; 34(11):1655-65. ISSN 0090-6964.

Brown J.M., et al. Isolated aortic valve replacement in North America comprising 108,687 patients in 10 years: Changes in risks, valve types, and outcomes in the Society of Thoracic Surgeons National Database. J Thorac Cardiov Sur 2009; 137(1):8290. ISSN 0022-5223.

Cohn M.D., Lawrence H., Daniel M.D., Sary F. Aranki. One Thousand Minimally Invasive Valve Operations. Ann Surg. 2004; 240(3): 529–534.

Colazzo F., et al. Extracellular matrix production by adipose-derived stem cells: Implication for heart valve tissue engineering. Biomaterials 2011; 32: 119-27. ISSN 0142-9612.

Filova, E., et al. Improved adhesion and differentiation of endothelial cells on surface-attached fibrin structures containing extracellular matrix proteins. J Biomed Mater Res A. 2014;102(3):698-712. ISSN 1552-4965.

FlexCell International Corporation, 2016, URL:http://store.flexcellint.com/bioflexplate.html

Ghodsizad A., et al. Magnetically guided recellularization of decellularized stented porcine pericardium derived aortic valve for TAVI. ASAIO J. 2014 Jul 3. ISSN 1538-943X

Golczyk K., Kompis M., Englberger L., Carrel TP., Stalder M. Heart valve sound of various mechanical composite grafts, and the impact on patients' quality of life. The Journal of heart valve disease 19 (2): 228–232. PMID 20369508. Retrieved December 7, 2012.

Griffths L.G., et al. Protein extraction and 2-DE of water- and lipid-soluble proteins from bovine pericardium, a low-cellularity tissue. Electrophoresis. 2008;29(22),4508-15. ISSN 1522-2683.

Lanza R., Langer R., Vacanti J., Principles of Tissue Engineering, ed. 3rd Edition , Elsevier Academic Press, 2007, ISBN 978-0123706157.

Joseph D. Bronzino. The Biomedical Engineering Handbook,, ed. I. ed, Boca Raton : CRC Press, c2000. ,2000, ISBN 0-8493-0461-X

McGowan K. Semiconductors: from book to breadboard, Delmar CENGAGE Learning, 2012 John G. Webster. , The measurement, instrumentation and sensors handbook, ed. (The Electrical engineering handbook series), Boca Raton : CRC Press, 1999, ISBN 9780471676003.

Havlikova J., et al. Network formation and differentiation of adipose-derived stromal cells in fibrin matrices J.Angiogenesis 2014; 17(1):302-302. ISSN 2040-2384.

Hibbeler R.C., Engineering mechanics, 13th Edition, Pearson, 2013. p. 678. ISBN 13: 978-0-13-291554-0. Ku, C.H., et al. Collagen synthesis by mesenchymal stem cells and aortic valve interstitial cells in response to mechanical stretch. Cardiovasc. Res. 2006;71:548-556. ISSN 1755-3245.

Matejka R., et al. IEEE conference proceedings. 4th IEEE International Conference on e-Health and Bioengineering EHB 2013 . : Gr. T. Popa University of Medicine and Pharmacy, 2013. p. 14. ISBN 978-1-4799-2372-4.

Piper C., Hetzer R., Körfer R. The importance of secondary mitral valve involvement in primary aortic valve endocarditis; the mitral kissing vegetation. Eur Heart J. 2002; 23(1):79-86.

Policha A., et al. Endothelial differentiation of diabetic adipose-derived stem cells. J Surg Res. 2014 Jul 5.pii: S0022-4804(14)00619-2. doi: 10.1016/j.jss.2014.06.041. ISSN 0022-4804.

STREX Cell Strain Instrument User Manual (2016), URL: http://sydney.edu.au/ medicine /bosch/facilities/molecular-biology/live-cell/usermanual_ST14004%20with%20 transformer_ 052708.pdf

Teebken O.E., et al. Preclinical Development of Tissue Engineered Vein Valves and Venous Substitutes using Re-Endothelialised Human Vein Matrix. Eur. J. Vasc. Endovasc. Surg. 2009;37(1), 92-102. ISSN1078-5884.

Yankah C.A., Weng Y.G., Hetzer R., Aortic Root Surgery: The Biological Solution, Springer Science and Business Media, 2010.

Datasheets of electronic components

AD623 amplifier, URL: http://www.analog.com/media/en/technical-documentation/data-sheets/AD623.pdf
ADS1115 analog-to-digital convertor, URL: http://www.ti.com/lit/ds/symlink/ ads1115.pdf
LM317 three-terminal adjustable regulator, URL: http://www.ti.com/lit/ds/symlink/ lm317.pdf
LM4132 voltage reference, URL: http://www.ti.com.cn/cn/lit/ds/symlink/lm4132.pdf
TLC271 operational amplifier, URL: http://www.ti.com/lit/ds/symlink/tlc271.pdf
ZVN2106 transistor, URL: http://www.diodes.com/_files/datasheets/ZVN2106G.pdf

List of Figures

List of Tables

Appendices

Appendix A - Pressure sensor electrical design

Electrical circuit diagram

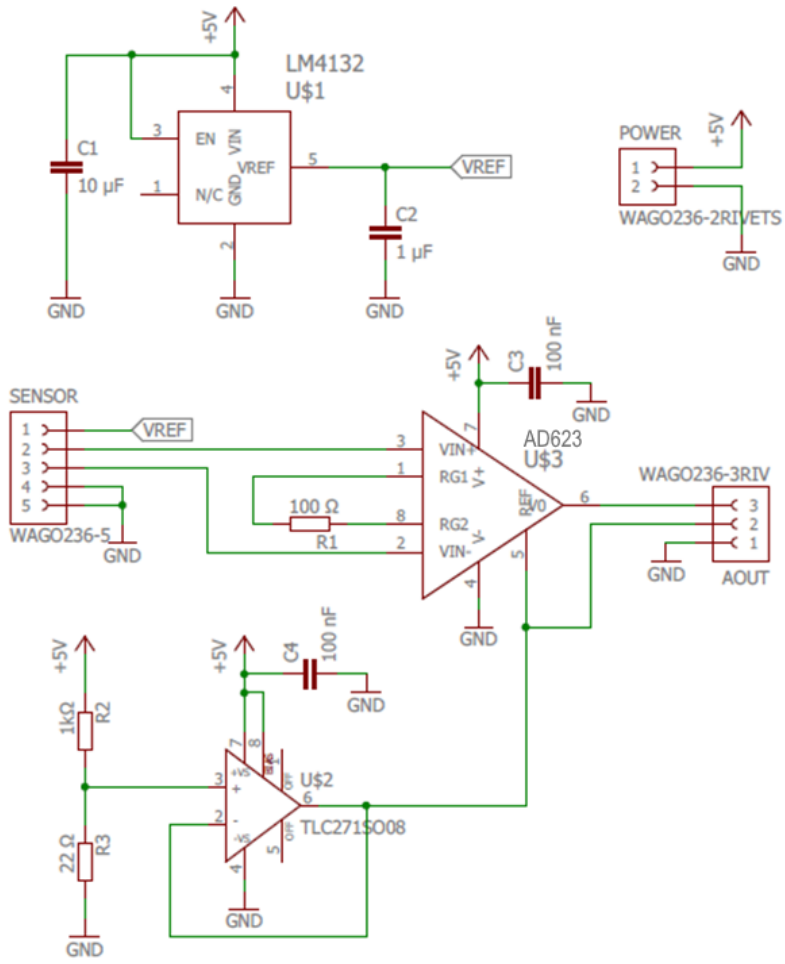

Printed circuit board

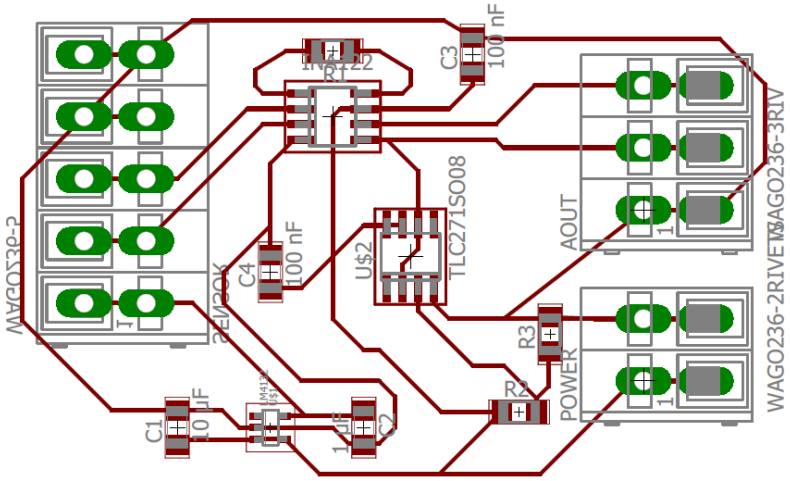

Nominals of electronic elements:

$R1 = 150\ \Omega$

$R2 = 1\ \text{k}\Omega$

$R3 = 22\ \Omega$

$C1 = 10\ \mu\text{F}$

$C2 = 1\ \mu\text{F}$

$C3 = C4 = 100\ \text{nF}$

Appendix B - Extension sensor electrical design

Electrical circuit diagram

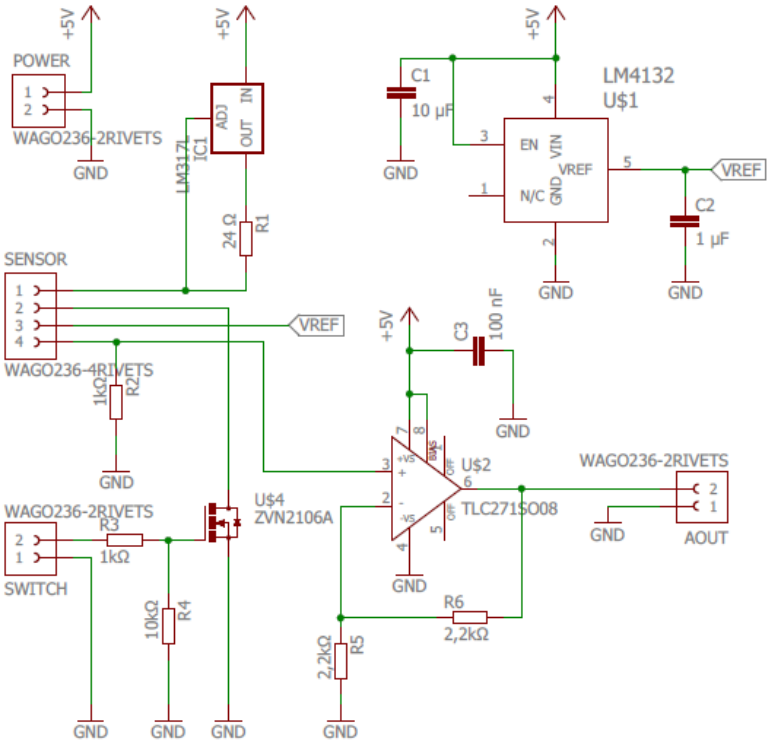

Printed circuit board

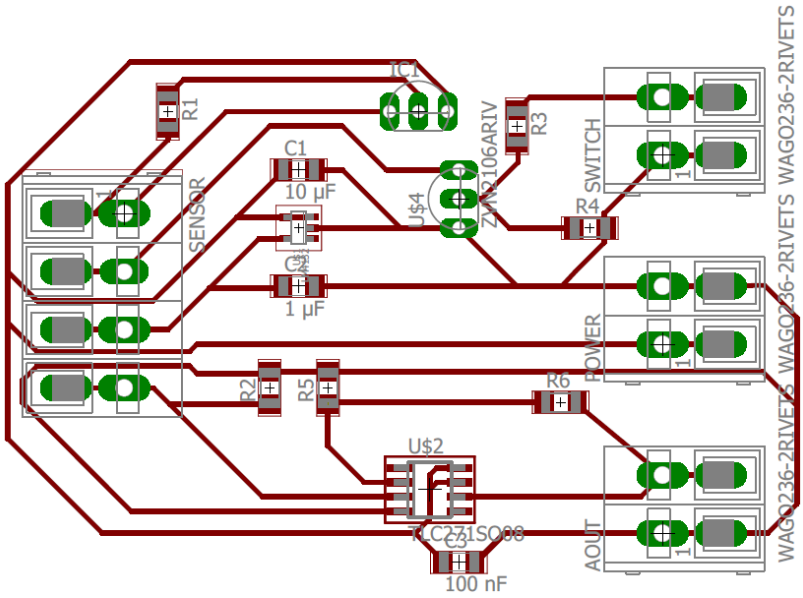

Nominals of electronic elements:

$R1 = 24\ \Omega$

$R2 = 1\ \text{k}\Omega$

$R3 = 1\ \text{k}\Omega$

$R4 = 10\ \text{k}\Omega$

$R5 = R5 = 2{,}2\ \text{k}\Omega$

$C1 = 10\ \mu\text{F}$

$C2 = 1\ \mu\text{F}$

$C3 = 100\ \text{nF}$

Appendix C - ADS1115. Electrical design

Electrical circuit diagram

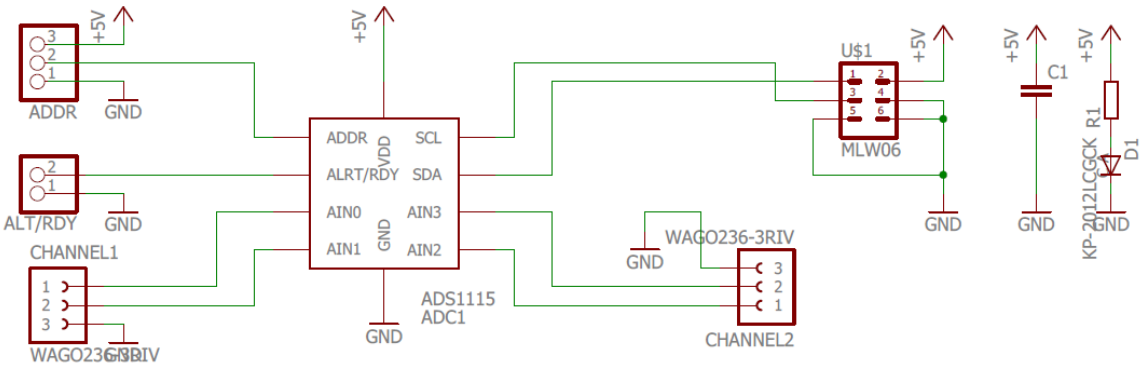

Printed circuit board

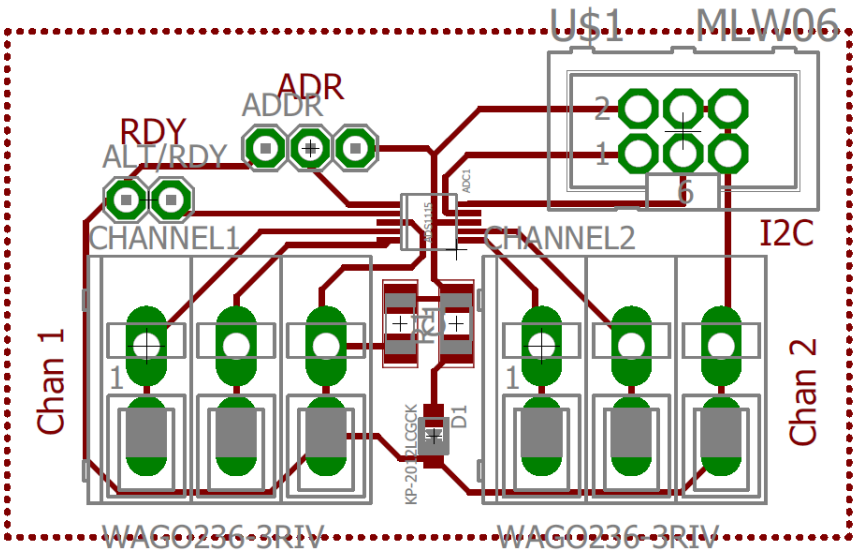

Nominals of electronic elements:

$R1 = 1\ \text{k}\Omega$

$C1 = 100\ \text{nF}$

Appendix D - 24V-to-5V transformer. Electrical design

Electrical circuit diagram

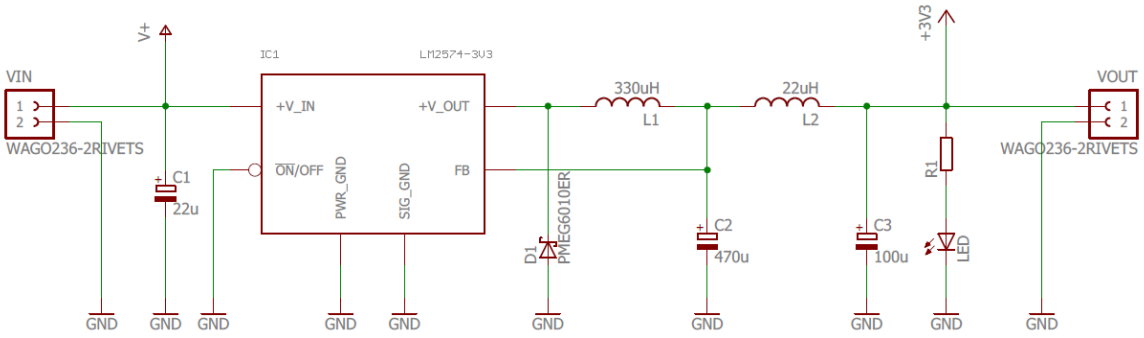

Printed circuit board

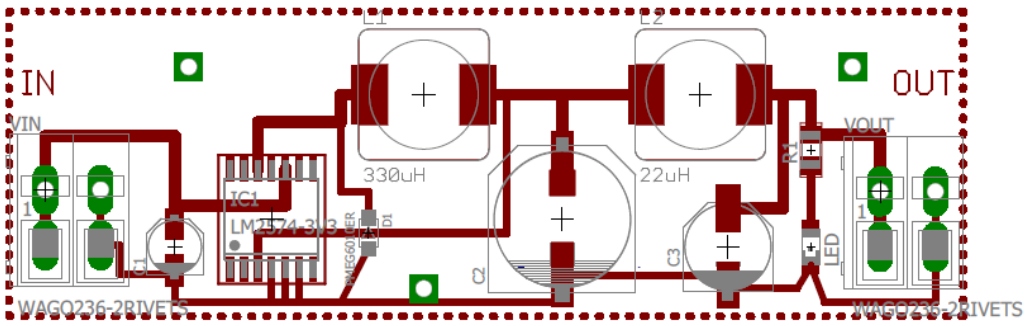

Nominals of electronic elements:

$R1 = 1\ \text{k}\Omega$

$C1 = 22\ \mu\text{F}$

$C2 = 470\ \mu\text{F}$

$L1 = 330\ \mu\text{F}$

$L2 = 22\ \mu\text{H}$

Appendix E - Extension sensor's calibration protocols

Preliminary extension sensor calibration. All values are in millivolts. Time of the calibration measurements: 13:00-18:00, daylight, room lights off.

h, mm	nothing**	nothing repetition	nothing*	sticker	sticker*	white band	white band*	black band
1	200,07	214,73	157,92	1823,31	1782,30	1221,48	1192,16	146,07
2	136,75	170,13	120,75	1403,23	1357,54	878,78	827,96	84,63
3	103,82	144,07	83,82	1094,53	1044,84	686,83	631,34	58,88
4	94,63	122,50	74,88	828,40	765,65	530,39	470,09	44,69
5	92,13	115,13	67,19	663,58	595,68	427,89	353,76	32,88
6	86,19	107,82	58,44	568,70	485,20	338,45	263,01	26,56
7	81,35	102,07	54,38	447,97	368,64	304,38	226,69	21,06
8	75,41	99,50	52,06	375,57	294,07	261,88	184,76	19,81
9	72,69	95,50	50,56	323,28	242,19	232,82	153,13	18,00
10	69,89	92,57	42,06	283,45	201,26	209,44	131,75	17,19
11	67,63	89,32	38,94	252,63	172,19	185,82	109,94	17,19
12	64,75	88,25	39,13	228,38	149,38	171,01	97,13	17,63
13	59,69	84,07	29,15	203,26	128,32	155,19	83,53	18,69
14	56,88	77,99	24,94	182,26	110,57	142,75	73,13	20,38

h, mm	black band*	silicon transparent	silicon transparent*	silicon non-transparent	silicon non-transparent*	chamber material	chamber material*
1	144,13	404,32	352,57	1847,24	1821,47	223,57	160,82
2	83,32	268,63	210,76	1387,48	1367,47	162,19	98,94
3	56,88	216,26	155,32	1100,41	1068,72	137,25	75,88
4	42,38	187,57	130,25	797,34	729,96	117,75	58,50
5	30,06	163,94	116,16	652,08	578,33	106,63	50,75
6	23,25	148,94	91,32	547,89	463,95	104,38	46,56
7	17,19	134,75	80,81	452,51	366,70	99,32	38,06
8	15,44	126,25	59,94	381,64	293,38	97,88	37,63
9	12,50	119,25	52,56	338,45	246,88	95,07	35,06
10	10,81	116,25	56,25	299,95	215,07	89,57	29,50
11	9,81	106,75	47,94	277,38	193,94	88,69	27,06
12	9,31	98,88	39,13	250,01	171,01	89,07	26,50
13	9,31	96,25	42,44	222,63	144,57	85,19	26,94
14	9,00	88,57	35,88	204,19	122,57	82,94	25,56

Appendix F - Arduino microcontroller code

```
// OPTIONS SETUP
    // ADC I2C communication setups
    #include ¡Wire.h¿
    int ADC_Address = 0x48; // setting-up the address 100 1000
    int ADC_Config_Register = 0x01; // setting-up the addresses of inner registers 0000 0001
    int ADC_Pressure_MSB = 0x84; // setting-up the most significant byte for the channel 1 where the pressure signal comes
    int ADC_Pressure_LSB = 0x83; // setting-up the less significant byte for the channel 1 where the pressure signal comes
    int ADC_Extension_MSB = 0xB4; // setting-up the most significant byte for the channel 2 where the extension signal comes
    int ADC_Extension_LSB = 0x83; // setting-up the less significant byte for the channel 2 where the extension signal comes
    float ADC_Full_Scale = 2.048; // (Volts) the above-stated setups tune the ADS1115 for the full scale of +/- 2V048
    // Sensor setups
    float sensivity = 0.005075; // sensivity of the sensor from the experiments (for MILLI-VOLTS range)
    float inputVoltage = 5.0; // iput supply voltage +5V or +3V3
    int sampleRate = 32768; // decimal sample rate of the ADS ˆ(n-1)
    const int zeroingPin = 7; // the pin for reset button
    const int ledPin = 13; // the number of the LED pin
    // Processing setup
    int nReadings = 5; // number of readings for averaging
    int flag = 0; // variable for averaging function either to show or not the result
    int nZeroingReadings=5; // number of readings for ZERO averaging
    float Pressure_Offset = 33.0; // because of the common voltage problem there is an offset in the pressure sensor values
```

int buttonState = 0; // variable for reading the zeroingButton status

//————————————————————————————

void setup()

pinMode(ledPin, OUTPUT); // initialize the LED pin as an output

pinMode(zeroingPin, INPUT); // initialize the zeroingButton pin as an input

Wire.begin(); // join i2c bus (address optional for master)

Serial.begin(9600); // start serial communication at 9600bps

//————————————————————————————

int ADC_Channel1_Pressure_Setup ()

// setting up the Config register

Wire.beginTransmission(ADC_Address); // first 7-bit I2C address followed by a low read/write bit

Wire.write(ADC_Config_Register); //points to Config register

Wire.write(ADC_Pressure_MSB); //MSB of the Config register to be written - setting the Channel 1 for the reading 128 SPS / FS +2V048

Wire.write(ADC_Pressure_LSB); //LSB of the Config register to be written - setting the Channel 1 / conversion mode/ no comparator

Wire.endTransmission();

delay(300); // to clear the saved result of the last conversion

// setting up the Pointer register

Wire.beginTransmission(ADC_Address); // first 7-bit I2C address followed by a low read/write bit

Wire.write(0x00); //points to Conversion register

Wire.endTransmission();

int ADC_Channel2_Extension_Setup ()

Wire.beginTransmission(ADC_Address); // first 7-bit I2C address followed by a low read/write bit

Wire.write(ADC_Config_Register); //points to Config register

Wire.write(ADC_Extension_MSB); //MSB of the Config register to be written - setting the Channel 2 for the reading 128 SPS / FS +2V048

Wire.write(ADC_Extension_LSB); //LSB of the Config register to be written - setting the Channel 2 / conversion mode/ no comparator

Wire.endTransmission();

delay(300); // to clear the saved result of the last conversion

Wire.beginTransmission(ADC_Address); // first 7-bit I2C address followed by a low read/write bit

Wire.write(0x00);

Wire.endTransmission();

int ADC_Data_Read_Out ()

// request reading from sensor // request 2 bytes from slave device

Wire.requestFrom(ADC_Address, 2); // first 7-bit I2C address followed by a high read/write bit

// receive reading from sensor

int sensorReading;

if (2 ¡= Wire.available()) // if two bytes were received

sensorReading = Wire.read(); // receive high byte (overwrites previous reading)

sensorReading = sensorReading ¡¡ 8; // shift high byte to be high 8 bits

sensorReading —= Wire.read(); // receive low byte as lower 8 bits

return sensorReading;

float zerReading = 0;

int j=-1;

int Zeroing_Button_Read_Out (float Current_Pressure)

// read the state of the pushbutton value:

buttonState = digitalRead(zeroingPin);

if (buttonState == HIGH) j=0; // if it is, the buttonState is HIGH, the flag is shifted to zero

if (j¿=0)

zerReading+=Current_Pressure;

j=j+1;

Pressure_Offset = zerReading/j;

digitalWrite(ledPin, HIGH);

if (j == nZeroingReadings)

zerReading = 0;

j = -1;

digitalWrite(ledPin, LOW);

int sumReading = 0;

int n=0;

float pressureAveraging(int sensorValue, int nReadings)

sumReading+=sensorValue;

n=n+1;

float x = sumReading/n;

if (n == nReadings)

sumReading = 0;

n = 0;

flag=1;

else flag = 0;

return x;

float VoltageScaling(float sensorReading)

float sensorVoltage;

sensorVoltage = ADC_Full_Scale*1000*sensorReading/(sampleRate-1); // calculating the current voltage value according to the ADC's sample rate and full scale

return sensorVoltage;

float PressureCalculation (float pressureVoltage)

float pressure;

pressure = pressureVoltage/(100*sensivity*inputVoltage); // calculating the pressure in mmHg

return pressure;

void PrintOutResults (int pressureReading,float averagedPressureVoltage,int flag, float pressureVoltage,float pressureValue, float pressureOffset, float pressureCorrected) //, float vA,float pA)

```
Serial.print("PDig: ");
Serial.print(pressureReading);
Serial.print(" —Vol: ");
Serial.print(pressureVoltage);
Serial.print(" mV");
Serial.print(" —PNor: ");
Serial.print(pressureValue);
Serial.print(" mmHg");
Serial.print(" —POff: ");
Serial.print(pressureOffset);
Serial.print(" mmHg");
Serial.print(" —PCorr: ");
Serial.print(pressureCorrected);
Serial.print(" mmHg");
if (flag==1)
Serial.print(" —Vav:");
Serial.print(vA);
Serial.print(" —Pav:");
Serial.print(pA);
float YoungsModulusCalculation(float pressure,float extension)
float ym; //declaring the young's modulus variable
ym = pressure/extension; //calculating the young's modulus variable
return ym;
void SendMessage(float pressureValue,float extensionValue)
int presInt;
presInt = pressureValue*100; // increasing the accuracy of the integer to 0.01
byte pressureMSB = presInt ¿¿ 8; // pressure values most significant byte
byte pressureLSB = presInt; // pressure values less significant byte
int exInt;
```

```
exInt = extensionValue*1000; // increasing the accuracy of the integer to 0.001
byte extensionMSB = exInt ¿¿ 8; // extension values most significant byte
byte extensionLSB = exInt; // extension values less significant byte
byte sendMessage[7];
sendMessage[0] = 0x02; // ¡STX¿ start of the text message
sendMessage[1] = pressureMSB; // pressure values most significant byte
sendMessage[2] = pressureLSB; // pressure values less significant byte
sendMessage[3] = extensionMSB; // pressure values most significant byte
sendMessage[4] = extensionLSB; // pressure values less significant byte
sendMessage[5] = 0x03; // ¡ETX¿ end of the text message
byte LRC = 0;
for (int i=0; i ¡= 5; i++)
LRC += sendMessage[i];
LRC ≙ 0xFF +1;
sendMessage[6] = LRC; // ¡LRC¿ redundancy check
Serial.write(sendMessage,7);  void loop()
////////////////////// PRESSURE SENSOR ////////////////
ADC_Channel1_Pressure_Setup ();
int pressureReading;
pressureReading = ADC_Data_Read_Out();
float averagedPressureVoltage;
averagedPressureVoltage = pressureAveraging(pressureReading, nReadings);
float pressureVoltage;
pressureVoltage = VoltageScaling(pressureReading);
float pressureVoltageAVERAGED;
pressureVoltageAVERAGED = VoltageScaling(averagedPressureVoltage);
float pressureValue;
pressureValue = PressureCalculation (pressureVoltage);
float pressureValueAVERAGED;
```

```
pressureValueAVERAGED = PressureCalculation (pressureVoltageAVERAGED);
Zeroing_Button_Read_Out(pressureValue);
float Pressure_Corrected = pressureValue-Pressure_Offset;
PrintOutResults(pressureReading, averagedPressureVoltage, flag, pressureVoltage, pressureValue, Pressure_ Offset, Pressure_Corrected);//, pressureVoltageAVERAGED, pressureValueAVERAGED);
//////////////////// EXTENSION SENSOR ////////////////////
ADC_Channel2_Extension_Setup ();
int extensionReading;
extensionReading = ADC_Data_Read_Out();
Serial.print("—— Ex: ");
Serial.print(extensionReading);
float extensionVoltage;
extensionVoltage = VoltageScaling(extensionReading);
Serial.print(" — EVol: ");
Serial.print(extensionVoltage);
Serial.print(" mV");
///////////////// YOUNGS MODULUS /////////////////////
float YoungsModulus;
YoungsModulus = YoungsModulusCalculation(pressureVoltage,extensionVoltage);
Serial.print(" — YM: ");
Serial.println(YoungsModulus);
///////////////// SEND MESSAGE /////////////////////
SendMessage(Pressure_Corrected,extensionVoltage);
```

Appendix G - 25-pin connector description

Pin 1 - SDA

Pin 2 - SCK

Pin 4 - Pressure sensor analog GND

Pin 5 - Pressure sensor analog positive output

Pin 6 - Pressure sensor analog negative output

Pin 9 - Extension sensor switch control (CNY70's LED on/off button. Input)

Pin 13 - +24 Volts rail for power supply

Pin 17 - Extension sensor analog GND

Pin 18 - Extension sensor analog positive output

Pin 19 - Extension sensor analog negative output

Pin 20 - Pressure sensor "Reset offset" button (Output)

Pin 25 - GND rail for power supply

Appendix H - Mechanical drawings

Adjustable mounting for the CNY70 holder

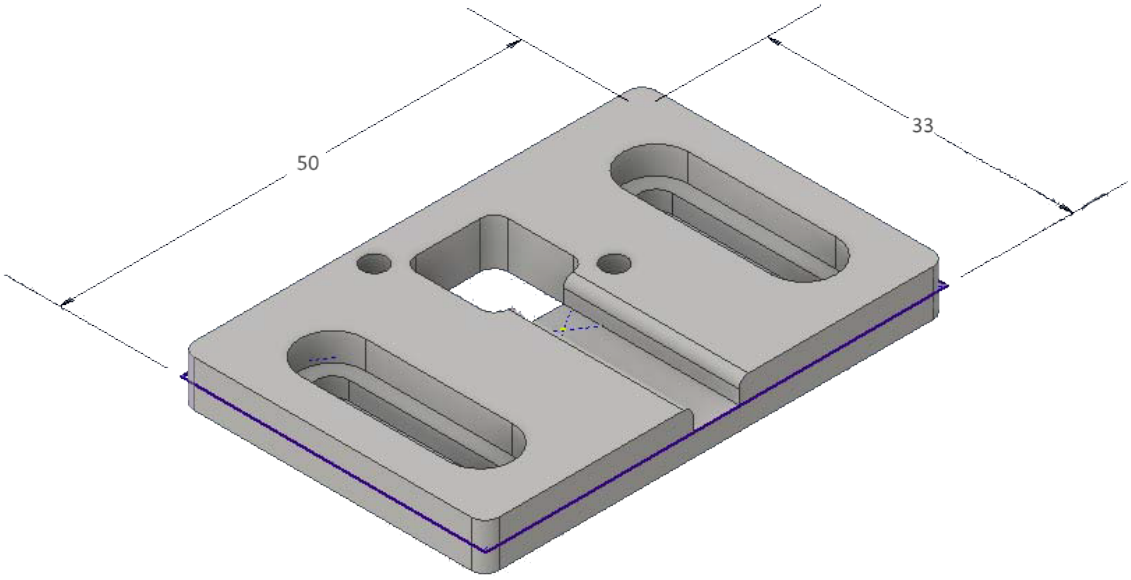

CNY70 holder

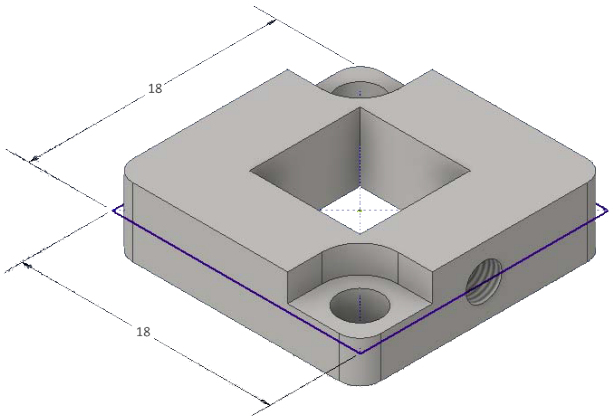

Stand-plate of the cultivation chamber